

## **General Disclaimer**

### **One or more of the Following Statements may affect this Document**

- This document has been reproduced from the best copy furnished by the organizational source. It is being released in the interest of making available as much information as possible.
- This document may contain data, which exceeds the sheet parameters. It was furnished in this condition by the organizational source and is the best copy available.
- This document may contain tone-on-tone or color graphs, charts and/or pictures, which have been reproduced in black and white.
- This document is paginated as submitted by the original source.
- Portions of this document are not fully legible due to the historical nature of some of the material. However, it is the best reproduction available from the original submission.

**ORBITAL TRANSFER AND RELEASE  
OF TETHERED PAYLOADS**

**CONTINUATION OF  
INVESTIGATION OF ELECTRODYNAMIC STABILIZATION AND  
CONTROL OF LONG ORBITING TETHERS**

Contract NAS8-33691

**ORIGINAL PAGE IS  
OF POOR QUALITY**

**Final Report**

**For the period 1 September 1979 thru 28 February 1983**

**Principal Investigator**

**Dr. Giuseppe Colombo**

**March 1983**

**Smithsonian Institution  
Astrophysical Observatory  
Cambridge, Massachusetts 02138**

**The Smithsonian Astrophysical Observatory  
is a member of the  
Harvard-Smithsonian Center for Astrophysics**



**(NASA-CR-170779) ORBITAL TRANSFER AND  
RELEASE OF TETHERED PAYLOADS. CONTINUATION  
OF INVESTIGATION OF ELECTRODYNAMIC  
STABILIZATION AND CONTROL OF LONG ORBITING  
TETHERS (Smithsonian Astrophysical**

**N83-25751**

**Unclas  
G3/15 03796**

**ORBITAL TRANSFER AND RELEASE  
OF TETHERED PAYLOADS**

**CONTINUATION OF  
INVESTIGATION OF ELECTRODYNAMIC STABILIZATION AND  
CONTROL OF LONG ORBITING TETHERS**

**Contract NAS8-33691**

**Final Report**

**For the period 1 September 1979 thru 28 February 1983**

**Principal Investigator**

**Dr. Giuseppe Colombo**

**Co-Investigators**

**Dr. Mario D. Grossi**

**Mr. David Arnold**

**Dr. Manuel Martinez-Sanchez  
Massachusetts Institute of Technology**

## Table of Contents

1.0 Introduction . . . . .	
2.0 Summary . . . . .	
3.0 Changes in Mean Altitude of Tethered Satellite System	
During Retrieval . . . . .	
3.1 Analytical Study . . . . .	
3.2 Computer Simulation . . . . .	
4.0 Release of a Heavy Payload From the End of the Tether . . . . .	
4.1 Discussion of Approach . . . . .	
4.2 Results of Study . . . . .	
Appendix A. Tethers for Orbital Transfer and Satellite	
Servicing. Final Report to SAO (Subcontract SV2-52005)	
by The Space Systems Laboratory (MIT) dated 1 April	
1983. . . . .	



List of Figures

Figure 4-1. Payload release using a half-period sinusoid: three mass point model. Amplitude (length of tether reeled in during maneuver) = 933 meters, period = 104.7 seconds, release time = 141.8 seconds from start of maneuver. (a) Tension between mass points vs. time (b) radial vs. in-plane configuration: mass point spacing 1.5 km to show motions.

Figure 4-2. Payload release using a half-period co-sinusoid: five mass point model. Amplitude = 533 meters, period = 209 seconds, release time = 230 seconds, reeling maneuver stop = 104.7 seconds. (a) Tension between mass points vs. time (b) radial vs. in-plane behavior: mass point spacing 2 km to show motions.

Figure 4-3. Payload release using a full-period co-sinusoid five mass model. Amplitude = 454 meters, period = 139 seconds, release time = 159 seconds from start of maneuver. (a) Tension between mass points vs. time (b) radial vs. in-plane behavior: mass point spacing 1 km to show motions.

Figure 4-4. Payload release using a full-period co-sinusoid: ten mass point model. All parameters of run and figure same as Figure 4-3 (a) tension vs. time, (b) radial vs. in-plane behavior.

Figure 4-5. Payload release using a full period co-sinusoid: ten mass point model with 3 mm diameter kelvar tether replacing 2 mm diameter tether used in previous runs. Other parameters same as Figure 4-3 and 4-4. Tension vs. time, (b) radial vs. in-plane behavior.

List of Tables

Table 4-1. Post Retrieval Altitudes of Tethered Systems.

## 1.0 Introduction

SAO studied a variety of tether dynamic and electrodynamic issues under this contract, NAS8-33691, beginning in September 1979. This work is the foundation upon which present and future tether dynamics studies rest. Results are detailed in the following reports:

"The Skyhook Program: A Software Package for a Tethered Satellite System, Including Electrodynamic Interactions" (May 1980 - Reprinted October 1982 as Special Projects Group Technical Report TP80-01).

"Investigation of Electrodynamic Stabilization and Control of Long Orbiting Tethers" (March 1981).

"The Use of Tethers for Payload Orbital Transfer" (March 1982).

"Study of Certain Tether Safety Issues" (March 1982).

"Study of Tethered Satellite Active Attitude Control (October 1982).

This work was performed under Dr. Giuseppe Colombo, Principal Investigator. Mr. David A. Arnold was Chief Analyst and Co-Investigator. Dr. Mario D. Grossi, Radiophysicist, was also a Co-Investigator and contributed to the electrodynamic studies. The "Use of Tethers for Payload Orbital Transfer" included work at the Massachusetts Institute of Technology (MIT), under Dr. Manuel Martinez-Sanchez, Co-Investigator.

The present report covers work at SAO and MIT during the period 1 September 1982 through 28 February 1983 regarding (at SAO) reel motor contributions to tether system total energy during payload retrieval and the development of control laws for stable release of tether deployed massive payloads and (at MIT) space-based tethers for orbital

transfer and satellite servicing. Dr. Martinez-Sanchez headed the effort at MIT. The work was managed by Richard S. Taylor at SAO. The authors of this report are Mr. David A. Arnold, Dr. Manuel Martinez-Sanchez, and Mr. Richard S. Taylor.

## 2.0 Summary of Study, Conclusions, and Recommendations

### Summary

This section presents, on the following pages, highlights of the study in the three areas of research undertaken.

- 1) The effect of reeling operations on the orbital altitude of the tether system.
- 2) The development of control laws to minimize tether rebound upon payload release.
- 3) The use of the tether for LEO/GEO payload orbital transfer.

Details of the study are given in the succeeding sections of the report and in the Appendix.

### Conclusions

As a result of this work, we conclude that:

- 1) Reeling operations can contribute a significant amount of energy to the orbit of the system and should be considered in orbit calculations and predictions.
- 2) Deployment of payloads, even very large payloads, using tethers is a practical and fully stable operation.
- 3) Tether augmented LEO/GEO transfer operations yield useful payload gains under the practical constraint of fixed size OTV's.
- 4) Orbit-to-Orbit satellite retrieval limited by useful revisit times to orbital inclinations of less than forty-five degrees.

### Recommendations

Further evaluation of the payload orbital transfer concept demonstrated as feasible in this study will lead to a full understanding of the capabilities of the approach. It is necessary to consider the practical limitations imposed by reasonable tether lengths and masses, to determine the capabilities and requirements of the release end teleoperator, and to determine its efficiency in comparison to OTV techniques, particularly in achieving payload orbit circularization from an elliptical Shuttle orbit. Payload gains to GEO have been demonstrated in this study. It is reasonable to expect similar gains in lower Earth orbit operations.

EFFECT OF REELING OPERATION  
ON  
ORBITAL ALTITUDE  
OF THE TETHER SYSTEM

ORIGINAL PAGE IS  
OF POOR QUALITY

- STUDIED RETRIEVAL USING TWO EQUAL MASSES AND A MASSLESS TETHER.
- REEL MOTOR ENERGY CONTRIBUTION ADDS TO SYSTEM ENERGY.
- POST-RETRIEVAL SYSTEM ALTITUDE ALWAYS IS GREATER THAN INITIAL CENTER-OF-MASS ALTITUDE.
- POST-RETRIEVAL SYSTEM ALTITUDE CAN BE GREATER THAN INITIAL UPPER MASS ALTITUDE IN THIS IDEALIZED CASE.



Energy contributed to the system during retrieval, or taken from it during deployment, significantly affects orbital altitude. For tethers longer than about 3000 km, the system studied: two equal masses with a massless tether, actually-- was able to "pull itself up by its own boot-straps" to above the initial altitude of the upper mass. This effect, while smaller, occurs in deployment and retrieval operations from the Space Shuttle and is significant for large (10 ton) deployed payloads and realistic tether lengths. It may also be a factor in orbital calculations with small (0.5 ton) payloads such as will be deployed by the TSS facility. Inclusion of tether mass in the calculation significantly reduces the altitude gains obtained (see text).

ORIGINAL PAGE IS  
OF POOR QUALITY

ALAN SKYHOOK  
12:52:54 9 DEC 1982



Smithsonian Astrophysical Observatory

# PAYLOAD RELEASE STUDY TENSION VS. TIME

MODEL UNDER INVESTIGATION

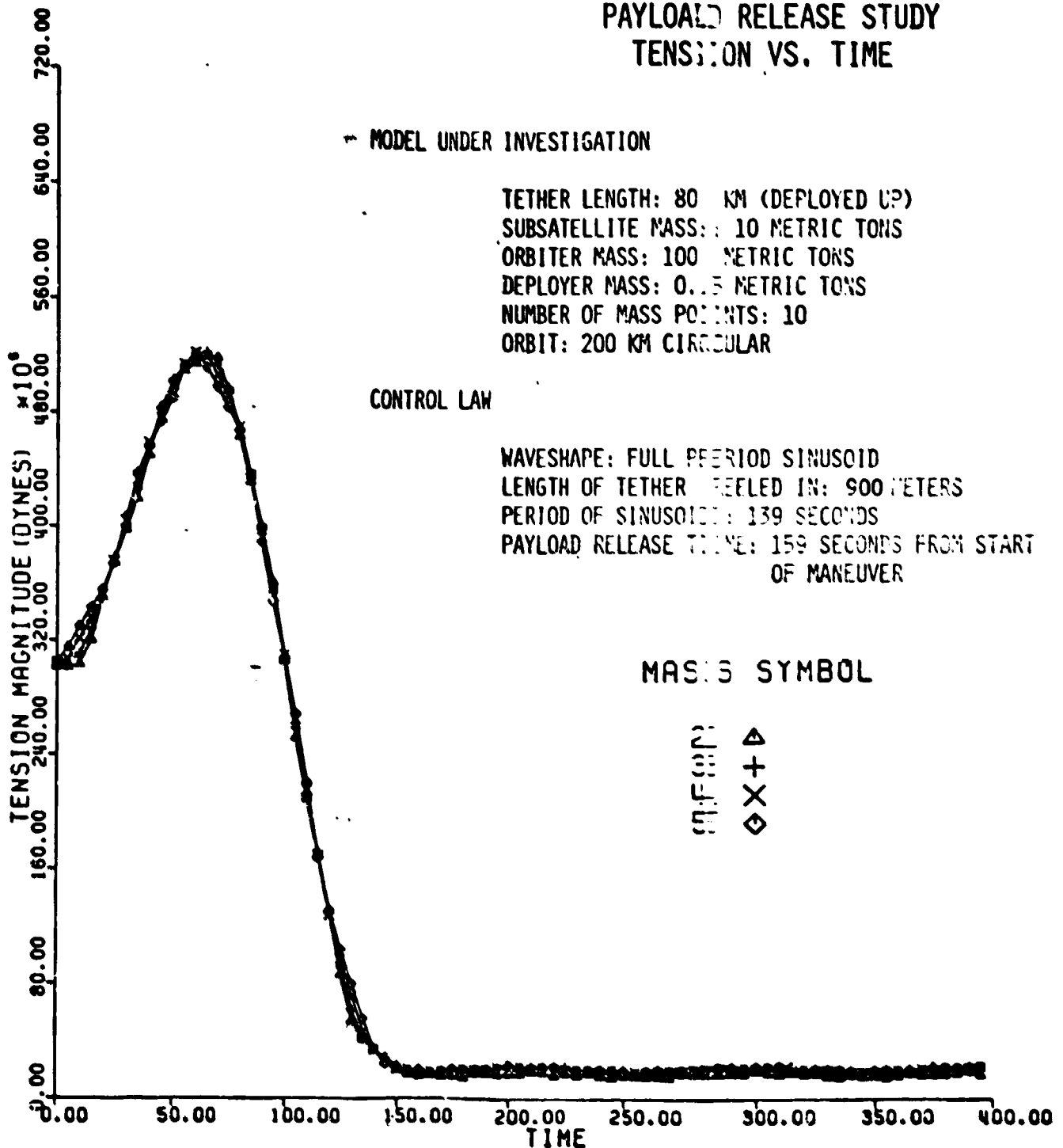
TETHER LENGTH: 80 KM (DEPLOYED UP)  
SUBSATELLITE MASS: 10 METRIC TONS  
ORBITER MASS: 100 METRIC TONS  
DEPLOYER MASS: 0.5 METRIC TONS  
NUMBER OF MASS POINTS: 10  
ORBIT: 200 KM CIRCULAR

CONTROL LAW

WAVESHAPE: FULL PERIOD SINUSOID  
LENGTH OF TETHER REELED IN: 900 METERS  
PERIOD OF SINUSOID: 139 SECONDS  
PAYLOAD RELEASE TIME: 159 SECONDS FROM START  
OF MANEUVER

MASS SYMBOL

INFO  
△  
+  
X  
◇



11 DECEMBER 1982



This figure and the one following present the most important result of this study: that stable deployment of large payloads (10 ton range) is possible using tethers. Displaying tether tension as a function of time clearly shows the effect of the reeling maneuver on the system. Reel-in causes an initial increase in tension followed by an immediate dip to the projected post-release tension. Payload release at 159 seconds leads to maintenance of the post release tension attained through the maneuver with only relatively small post release tension oscillation. Tension plots for the five mass points used in this run are overlapped in this figure. Propagation delays in the tether account for the curve spacing seen at each of the "turn arounds" in the curves. Tether tension remains above zero at all times during and subsequent to the maneuver.

ALAN SKYHOOK  
13:09:52 9 DEC 1982

PAYLOAD RELEASE STUDY  
RADIAL VS. IN-PLANE  
BEHAVIOR

MODEL UNDER INVESTIGATION

TETHER LENGTH: 80 KM (DEPLOYED UP)  
SUBSATELLITE MASS: 10 METRIC TONS  
ORBITER MASS: 100 METRIC TONS  
DEPLOYER MASS: 0.5 METRIC TONS  
NUMBER OF MASS POINTS: 10  
ORBIT: 200 KM CIRCULAR

CONTROL LAW

WAVESHAPE: FULL PERIOD SINUSOID  
LENGTH OF TETHER REELED IN: 900 METERS  
PERIOD OF SINUSOID: 139 SECONDS  
PAYLOAD RELEASE TIME: 159 SECONDS FROM START  
OF MANEUVER

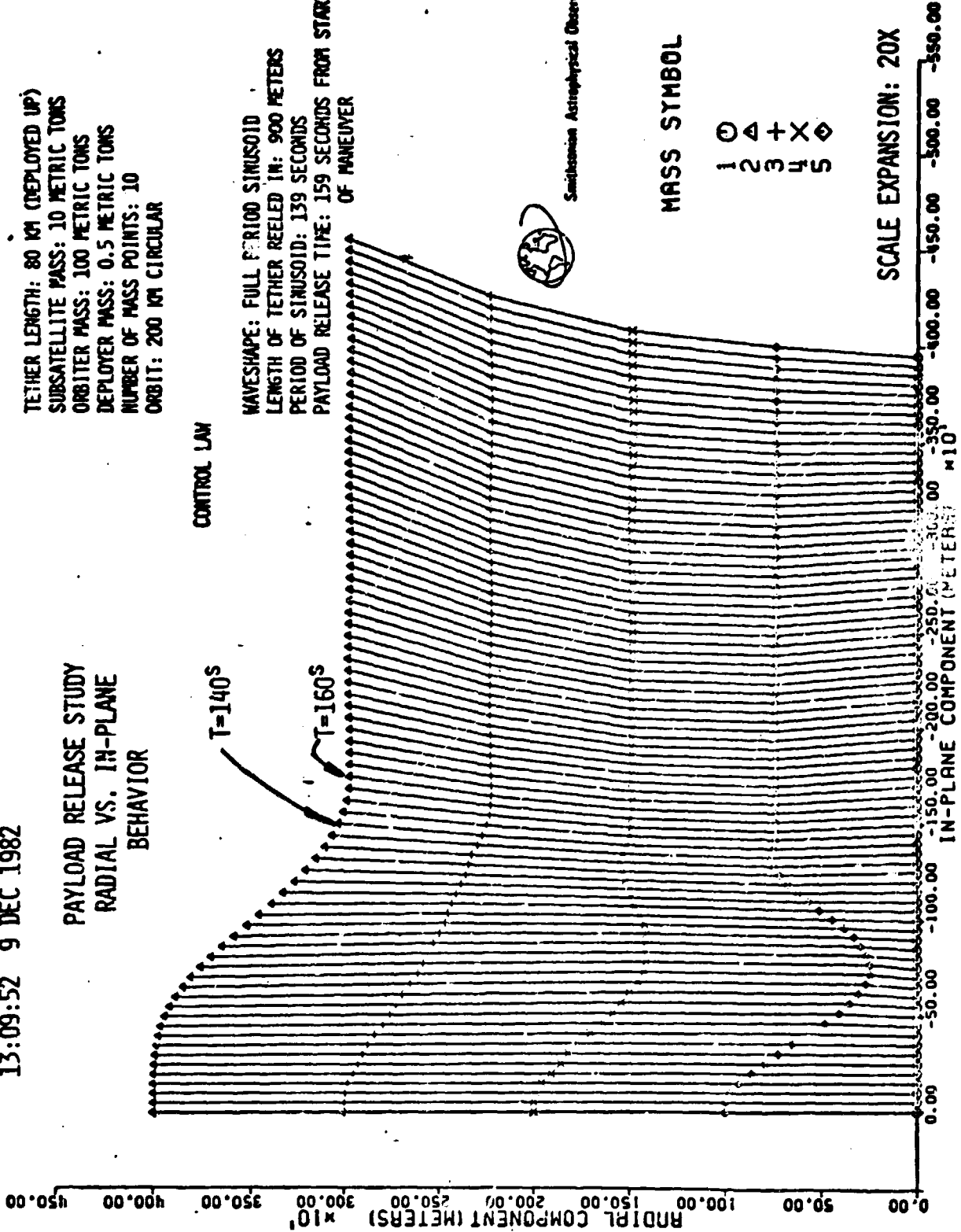


Swissair Astronautical Observatory

MASS SYMBOL

- 1 ○
- 2 △
- 3 +
- 4 X
- 5 ◇

SCALE EXPANSION: 20X



13 DECEMBER 1982

Here the radial vs. in-plane behavior (a "side view") of the system during the deployment is shown. A mass point spacing of 1 km was selected for use in the plot to expand both the vertical and horizontal scales twenty times and clearly show the behavior of the tether during the maneuver. The orbiter is the bottom mass point, the subsatellite the top mass point. Motion of the released payload is not shown. Shuttle motion is to the right. Tether configuration is plotted every five seconds with each plot displaced to the right .1 inches for clarity. In an unexpanded plot no tether motion would be observed. This run used a 2 mm diameter Kevlar tether; a 3 mm tether is actually necessary to insure an adequate margin of safety (see Figure 4-5).

Since stable deployment of large payloads by tethers is possible, it is essential to continue study of this issue to fully define the capabilities and requirements of the system. For instance, the maximum payload release mass with reasonable tether diameters and lengths, the capabilities and requirements to be placed on the release and teleoperator (mass, thrusting capability, etc.), and the efficiency of the system in relation to OTV use must be determined.

TETHERS FOR ORBITAL TRANSFER  
AND  
SATELLITE SERVICING

ORIGINAL PAGE IS  
OF POOR QUALITY

Page 15

TRANSFER MODE	CONDITIONS	COMMENTS	RESULTS
I. Ground to Orbit: Carry Tether Deployer on Shuttle - Payload to GEO	1. "Variable" OTV 2. Reduced OMS Load 3. LOX-LH <sub>2</sub> OTV's	Idealized Case - Maximizes Payload to GEO Under All Parameter Variations	No Advantage to Tether Deployment
II. Ground to Orbit: Shuttle Rendezvous with Tether Deployer In-Orbit - Payload to GEO	1. "Variable" OTV 2. Fixed Size OTV	Idealized Case	Some Increase in GEO Payload  Definite Gain in GEO Payload
III. Ground to Orbit: Carry Tether Deployer on Shuttle - Payload to Jupiter	1. Centaur OTV (4 Versions) Used in Study		Payload Gains of 280 Kg With Small Centaur's. Throw Weight Limitations Preclude Use of Larger Centaurs
IV. Orbit-to-Orbit: Satellite Retrieval	Satellites and Space Station at Different Altitudes But Same Inclination	Tether Lengths Up To 400 Km Considered	Differential Orbit Precession Rates Limit Usefulness to Inclinations Less Than About 45°. Below 45° Revisit Times Less Than One Year. For a Satellite at 700 Km and a Space Station at 300 Km.

Summary of M.I.T. Space Systems Laboratory Study  
Dr. M. Martinez-Sanchez



Smithsonian Astrophysical Observatory

Tether assisted payload orbital transfer provides payload gains to GEO and to a Jupiter interplanetary transfer orbit when an OTV of fixed size is considered. When the Shuttle carries an OTV to a tether deployer left orbiting as high as the maximum Shuttle OMS fuel capacity will allow. A payload gain of 12% per 100 km of tether is realized at GEO. In interplanetary transfer orbit injection, a payload gain of 280 kg is achieved which is a 34% gain with the smallest [D-15(R)] Centaur OTV and a 7% gain with the next largest (D-1T) Centaur. Tether assist provides either no or only minor payload gains when the deployer must be carried on each Shuttle mission or when the OTV capability can be configured for each mission to just meet the Shuttle throwweight capability.

Appendix A of this report is the MIT final report on this effort. It details the specific circumstances in which tether assisted deployment provides payload gains, provides further discussion of the satellite retrieval scheme, and considers tethered OTV-satellite rendezvous dynamics.

ORIGINAL PAGE IS  
OF POOR QUALITY

### 3.0 Changes in Mean Altitude During Retrieval

#### 3.1 Analytical Study

Let us assume that a tethered satellite system is deployed and stabilized in a vertical configuration in a circular orbit. The condition of equilibrium for the system is

$$\int r \omega^2 dm = GM/dm/r^2 \quad (1)$$

where  $dm$  is an element of mass at distance  $r$  from the center of the earth,  $GM$  is the gravitational constant of the earth and  $\omega$  is the orbital angular velocity. The left side of the equation is the centrifugal force on the system and the right side is the gravitational attraction. Retrieval of the subsatellite requires that the reel motor do work on the system and therefore the orbital energy will not be constant. Assuming there is no propulsion, the angular momentum of the system must remain constant. The angular momentum  $L$  before retrieval is

$$L = \int r^2 \omega dm \quad (2)$$

The condition for equilibrium in a circular orbit after retrieval is

$$R\Omega^2 = GMm/R^2$$

or

$$\Omega^2 = GM/R^3 \quad (3)$$

where  $m$  is the total mass,  $R$  is the orbit radius, and  $\Omega$  is the orbital angular velocity. The angular momentum  $L$  after retrieval is

$$L = R^2 \Omega m \quad (4)$$

We want to solve for the orbit radius  $R$  after retrieval given  $dm$  as a function of  $r$  in the deployed state.

Solving equation (4) for  $\Omega$  gives

$$\Omega = L/mR^2 \quad (5)$$

Substituting equation (5) into equation (3) gives

$$L^2/m^2 R^4 = GM/R^3 \quad (6)$$

or

$$R = L^2/GMm^2 \quad (6)$$

Substituting the value of  $L$  from equation (2) into equation (6) gives

$$R = (\int r^2 dm)^2 \omega^2 / GMm^2 \quad (7)$$

Solving equation (1) for  $\omega^2$  we have

$$\omega^2 = (GM \int dm / r^2) / (\int r dm) \quad (8)$$

Substituting equation (8) into equation (7) gives

$$R = [(\int r^2 dm)^2 GM \int dm / r^2] / [GM m^2 \int r dm] = [(\int r^2 dm)^2 \int dm / r^2] / [m^2 \int r dm] \quad (9)$$

If the system is being represented by a set of discrete masses, the integrals can be replaced by sums to give

$$R = [(\sum r_i^2 m_i)^2 \sum m_i / r_i^2] / [(\sum m_i)^2 \sum r_i m_i] \quad (10)$$

The value of  $R$  obtained from this equation may be compared to the center of mass of the deployed system given by

$$CM = \int r dm / \int dm \quad (11)$$

Another measure of the center of the system is the point  $\bar{r}$  where the centrifugal and gravitational forces balance. This is given by

$$\bar{r} = (GM/\omega^2)^{1/3} \quad (12)$$

Substituting equation (8) into equation (12) gives

$$r = (\int r dm / \int dm / r^2)^{1/3} \quad (13)$$

### 3.2 Computer Simulation

A computer program has been written to calculate the final state after retrieval using the equations given in Section 3.1. In running the program for a variety of tether lengths it was discovered that the final altitude after retrieval can be greater than the altitude of the highest mass in the case of extremely long tethers. The case run was that of two equal masses connected by a massless tether. The situation of having the final altitude equal to the original altitude of the upper mass depends on the ratio of the orbital radii of the masses in the deployed state. By iteration, the critical ratio has been found to be 1.4513682256. This number is not exactly equal to any simple value such as  $\sqrt{2}$ . The result has been confirmed by setting  $m_1 = m_2$  and  $R = r_2$  in equation (10), above. Setting the masses equal gives

$$R = (r_1^2 m + r_2^2 m)^2 (m/r_1^2 + m/r_2^2) / [(2m)^2 (r_1 m + r_2 m)] \quad (14)$$

$$= (r_1^2 + r_2^2)^3 / [4 r_1^2 r_2^2 (r_1 + r_2)] \quad (14)$$



Setting  $R = r_2$  gives, after simplification

$$0 = r_1^6 + 3r_1^4 r_2^4 - 4r_1^3 r_2^3 - r_1^2 r_2^4 + r_2^6 \quad (15)$$

If we set  $r_1 = 1$ , and  $r_2 = r$ , the equation for the ratio of the radii is

$$0 = 1 + 3r^2 - 4r^3 - r^4 + r^6 \quad (16)$$

This equation is satisfied by the value  $r = 1.451368226$  obtained by iteration.

The total energy TE of the system is given by summing the kinetic and potential energy of each mass in the system. That is

$$TE = \sum_i (1/2 m_i v_i^2 - GMm_i/r_i) \quad (17)$$

where  $v_i$  is the velocity of the mass  $m_i$  at distance  $r_i$  from the center for the earth, and GM is the gravitational constant of the earth.

When the system is retrieved the total energy will increase as a result of the work done by the reel motor. The work W is given by

$$W = \int_{l=L}^0 T dl \quad (18)$$

where T is the tension is the instantaneous length and L is the total length. The change in total energy calculated from equation (17) before and after retrieval should be equal to the work calculated from equation (18). An exact solution of equation (18) would have to take into account the change in mean altitude of the system during retrieval and the non-linear dependence of tension on wire length. However for short tether lengths, the tension is given approximately by the expression

ORIGINAL PAGE IS  
OF POOR QUALITY  $T \sim 3GMx/r^3$

(19)

where  $x$  is the distance of an end mass from the orbital center of the system (defined as the point where there is no radial acceleration). Let us assume that the retrieval is done slowly so that equation (19) gives the tension at each stage of the retrieval. By symmetry, the work is twice the integral of the work done on either mass. Therefore we can write

$$W \sim 2 \int_{x=l/2}^0 3GMmx/r^3(-dx) = 3GMmL^2/(4r^3) \quad (20)$$

The program used to calculate the altitude after retrieval has been modified to calculate the change in total energy of the system and the work done by the reel motor using equation (20). This program has been run for a variety of initial altitudes of the masses. Table 4-1 gives the results of the runs.

$H_1$	$H_2$	$H_{cm}$	$\bar{H}$	$H_f$	$\Delta TE$	$W$
200	225	212.5	212.476	212.618	$.652702 \times 10^{14}$	$.652724 \times 10^{14}$
200	250	225	224.905	225.473	$.259583 \times 10^{15}$	$.259618 \times 10^{15}$
200	300	250	249.623	251.886	$.102635 \times 10^{16}$	$.102689 \times 10^{16}$
200	400	300	298.502	307.491	$.400962 \times 10^{16}$	$.401803 \times 10^{16}$
200	600	400	394.100	429.569	$.152762 \times 10^{17}$	$.154010 \times 10^{17}$
200	1000	600	577.096	715.555	$.551413 \times 10^{17}$	$.568683 \times 10^{17}$
200	1800	1000	913.591	1446.204	$.176493 \times 10^{18}$	$.197411 \times 10^{18}$
200	3400	1800	1490.810	3518.652	$.427558 \times 10^{18}$	$.628308 \times 10^{18}$
200	6600	3400	2386.392	10264.198	$.468826 \times 10^{18}$	$.181884 \times 10^{19}$

Table 4-1. Post Retrieval Altitudes of Tethered Systems

All altitudes are in kilometers, and energies are in dynes.  $H_1$  is the altitude of the lower mass,  $H_2$  is the altitude of the upper mass,  $H_{cm}$  is the center of mass,  $\bar{H}$  is the orbital center (point of zero acceleration),  $H_f$  is the final altitude after retrieval,  $\Delta TE$  is the increase in total energy and  $W$  is work calculated by equation (20).

To evaluate the effect of the mass of the tether, consider a tether of length  $l$  connecting two equal masses  $M$  in circular orbit. Let  $a$  be the radius of the circular orbit of the point  $C$ , the approximate center of mass, and which is close to the center of gravity of the system. We want to evaluate the lower limit for the mass of the tethers under the limitation that the stress of the tether can not be larger than a certain limit,  $\sigma$ , in the stable state which we will assume is  $50 \text{ kg w/mm}^2$  including a suitable safety factor.

We have

$$\tau = 3/2(g_0)(h/\sigma)M \quad (21)$$

where  $g$  is the acceleration of gravity at  $C$ . We assume that  $a = 6800 \text{ km}$ . The cross section of the tether should be

$$A = \tau/\sigma = 3/2 g (h/a)(M/\sigma) \quad (22)$$

The mass of the tether is

$$M_T = A h \mu = 3/2 (Mg/\sigma)(\mu) (h^2/a) = M \quad (23)$$

where  $\mu$  is the density taken to be  $\mu = 1.5 \text{ g/cm}^3$

The coefficient

$$M_T/M = \alpha = 3/2 (\mu g/\sigma) (h^2/a) \quad (24)$$

May be evaluated now

$h = 200 \text{ km}$	$\alpha = 9/34$
$h = 300 \text{ km}$	$\alpha = 81/136$
$h = 400 \text{ km}$	$\alpha = 34/36$
$h = 500 \text{ km}$	$\alpha = 81/34$
$h = 800 \text{ km}$	$\alpha = 144/34$

From this table we may conclude that the computation of the final state of the system which has been done using a very simple model should be redone taking into account the effect of the mass of the tether for tether lengths greater than a few hundred km. Including tether mass in the calculation will significantly reduce the altitude gains seen with the massless tether.

For short tether lengths and returning to massless tethers, the approximate formula for  $W$  agrees with  $\Delta E$  to almost 5 decimal places. As the tether length increases, the formula for  $W$  becomes inadequate as expected. The altitude  $H_f$  after retrieval may be compared to either  $H_{cm}$  or  $\bar{H}$ , giving slightly different results for the increase in mean altitude. The change in altitude is small for short tethers. The altitude at which  $H_f$  becomes greater than  $H_2$  is 3169 km since this is where the ratio of the orbital radii is equal to 1.451368. For the last two entries,  $H_f$  is greater than  $H_2$ . From a practical point of view we must restrict our attention to tethers not exceeding a few hundred kilometers, because for longer tethers the mass of the tether becomes significant.

In order to provide a direct verification of the altitude after retrieval, some numerical integrations have been done using the SKYHOOK program. The third case with a 100 kilometer tether has been

run in the retrieval mode on SKYHOOK. The algorithm in the SKYHOOK program caused a rather rapid reeling in of the wire such that the system started looping after a few thousand seconds. The damping in the algorithm prevented a buildup of angular velocity as the retrieval continued but gravity gradient stabilization was never regained. The retrieval was terminated after 54600 seconds when the tether length was down to 10 meters. The final orbit of the center of mass of the system had an eccentricity of  $2.1684 \times 10^{-4}$  and a semi-major axis corresponding to a mean altitude of 251.8865078 km. This is very close to the value of 251.8861960 km computed theoretically using conservation of angular momentum. The differences between the theoretically computed value and the result of numerical integration is due to the eccentricity of the orbit introduced by the rather rapid retrieval. Conservation of angular momentum requires that the quantity  $a(1-e^2)$  be constant. The theoretical value is for  $e = 0$ . Therefore we should have  $a_{\text{theo}} = a_{\text{num}} (1-e^2)$ . Adding 6378 km for the radius of the earth to the orbital altitudes above gives  $a_{\text{theo}} = 6629.8861960$  and  $a_{\text{num}} = 6628.8865078$ . Using  $e = 2.1684 \times 10^{-4}$  gives  $a_{\text{num}} (1-e^2) = 6629.8861961$  in agreement with the value for  $a_{\text{theo}}$ .

Some tests were done varying the parameters in the retrieval algorithm to understand why the retrieval was unstable. The problem resulted from the method used to calculate the equilibrium wire tension in the retrieval algorithm. The tension must of course be greater than the equilibrium value to achieve retrieval. Normally the system consists of a heavy Shuttle and a relatively small payload. The acceleration on each mass depends on the distance from the orbital center of the system which is usually close to the Shuttle. The algorithm computes the tension from the total length of the wire. In the case being run, the orbital center is in the middle of the wire since the masses are equal. The tension computed by the algorithm is therefore about a factor of two too large. The run has been redone with the parameters divided by two. This resulted in a slow stable retrieval. After 60,000 seconds the wire length was down to about .6 km. The eccentricity of the orbit of the center of mass was  $3.8694 \times 10^{-5}$  and the semi-major axis corresponds to an orbital altitude of 251.8861189 km. The eccentricity was lower by more than a factor of five due to the slower retrieval. Plots of the orbit of the center of mass during the retrieval show that the eccentricity is introduced at the beginning of the retrieval.

#### 4.0 Release of A Heavy Payload From the End of the Tether

##### 4.1 Discussion of Approach

One of the potential uses of the tether is for launching a payload into a higher orbit by deploying it from the Shuttle or a space station on a long tether and then releasing it. The release would cause a sudden loss of force on the end of the wire resulting in recoil of the launching mechanism remaining at the end of the wire. Some initial analyses were done previously to study methods of avoiding recoil and loss of tension in the wire after payload release. A maneuver with the reel motor was simulated which pulled the payload toward the Shuttle and released it while the wire was under a lower tension approximately equal to the equilibrium value for the remaining mass. The initial study of this technique is described in the report "Investigation of Electrodynamic Stabilization and Control of Long Orbiting Tethers," G. Colombo, March 1981. In that study the payload released was 10 tons and the mass remaining at the end of the wire was 0.5 tons. The tether end mass therefore decreases by a factor of twenty during the release. To avoid loss of tension, the reel maneuver used must reduce the tension to 5% of its original value with an uncertainty of less than 5% of the original value. In the initial study the maneuver was simulated by having the change in wire length given by the expression  $-Asin\omega t$  where  $\omega t$  goes from  $0^\circ$  to  $180^\circ$ . In the results presented in the referenced report there was loss of tension in some segments of the wire after release of the payload, but the general approach seemed promising.

The present study is aimed at refining the algorithm used in the reel maneuver so as to develop a workable pre-release maneuver with particular emphasis on accounting for propagation delay and the dynamics of the tether itself in order to release the payload with no loss of tension along the wire. The propagation delay is the time required for a sound wave to travel the length of the wire. In a solid material the velocity is  $\sqrt{E/\rho}$  where  $E$  is the elasticity and  $\rho$  is the density of the material. For Kevlar,  $E = 0.7 \times 10^{12}$  dynes-cm, and  $\rho = 1.5$  grams/cc; the speed of sound is about 6.8 km/sec. The propagation delay is therefore about 12 seconds for an 80 km wire. The physical properties of a braided kevlar line could be significantly different than the properties of a monofilament line and should be determined experimentally. The tether itself will oscillate as a result of a reeling maneuver and these oscillations will cause tension variations along the wire and at both ends.

The reel control algorithm can be defined in various ways. The previous study also contained some results obtained with a tension control algorithm. This technique gave low excitation of wire oscillations. However, such an algorithm does not give any direct control over wire length. The length control algorithm used in the previous study has the disadvantage that the beginning and ending of the reel maneuver are abrupt and result in needless excitation of wire oscillations. Two variations of the original length control algorithm have been tried in the present study both of which represent length as  $A(\cos \omega t - 1)$ . In the first case  $\omega t$  goes from 0 to  $360^\circ$ , and the maneuver pulls the wire in and then lets it out to the original length. In the second case,  $\omega t$  goes from 0 to  $180^\circ$  and the wire is



**ORIGINAL PAGE IS  
OF POOR QUALITY**

Page 28

only pulled in; the final wire length is shorter. In either case the rate of change of wire length is zero at the beginning and end of the maneuver so that the first derivative is continuous and there is less excitation of wire oscillations.

The objective of the reel maneuver is to pull the end mass toward the Shuttle and release the payload when the wire tension has been reduced to the value required for equilibrium after release. The reel maneuver must be completed before this minimum tension is achieved to avoid changing the tension after release. The period of the reel maneuver must therefore be shorter than the natural period of oscillation of the subsatellite at the end of the wire. In the previous study it was assumed that the equilibrium tension is proportional to the mass at the end. In the case of a heavy payload, this assumption is not adequate because the center of gravity of the system undergoes a significant shift after release and the tension depends on the distance from the center of mass. This effect has been accounted for in the present study with improved results.

The response of the end mass to the reel maneuver cannot be calculated in a simple way. The approach used in this study is to start with a simple two mass integration (neglecting wire dynamics). From the elastic properties of the wire we calculate the change in wire stretch required to bring the tension to the desired value for release of the payload. The amplitude of the reel maneuver is set to the desired change in wire stretch and a test run done with a two-mass model. If the amplitude of the response is so large so that the wire goes slack the amplitude is reduced in the next run to eliminate loss of tension. The first parameter optimized is the period of the reel

only pulled in; the final wire length is shorter. In either case the rate of change of wire length is zero at the beginning and end of the maneuver so that the first derivative is continuous and there is less excitation of wire oscillations.

The objective of the reel maneuver is to pull the end mass toward the Shuttle and release the payload when the wire tension has been reduced to the value required for equilibrium after release. The reel maneuver must be completed before this minimum tension is achieved to avoid changing the tension after release. The period of the reel maneuver must therefore be shorter than the natural period of oscillation of the subsatellite at the end of the wire. In the previous study it was assumed that the equilibrium tension is proportional to the mass at the end. In the case of a heavy payload, this assumption is not adequate because the center of gravity of the system undergoes a significant shift after release and the tension depends on the distance from the center of mass. This effect has been accounted for in the present study with improved results.

The response of the end mass to the reel maneuver cannot be calculated in a simple way. The approach used in this study is to start with a simple two mass integration (neglecting wire dynamics). From the elastic properties of the wire we calculate the change in wire stretch required to bring the tension to the desired value for release of the payload. The amplitude of the reel maneuver is set to the desired change in wire stretch and a test run done with a two-mass model. If the amplitude of the response is so large so that the wire goes slack, the amplitude is reduced in the next run to eliminate loss of tension. The first parameter optimized is the period of the reel

maneuver so that the maneuver finishes, with an adequate margin, before the minimum wire tension is achieved. The payload release is not included in these runs which we made for determining the time of the minimum in the tension curve. For the two-mass model, either the tension or wire length can be used to determine the release time since the tension is linearly related to the wire length. Once the period is optimized, the amplitude is optimized by assuming that the response of the payload (that is, the change in distance from the Shuttle to the payload) is proportional to the amplitude of the reel maneuver. This assumption appears to be a good one when there is no loss of tension and the period of the reel maneuver is less than the natural period for longitudinal oscillations of the payload at the end of the wire. With the period and amplitude optimized, the payload is released and the tension variations examined in the post release time period. Very good results have been obtained for the tension fluctuations in the two-mass model since wire dynamics are neglected. In principle the tension fluctuations could be made arbitrarily small in the two-mass case by iterating the amplitude of the reel maneuver. In attempting to eliminate any tension variations after release it was found that the release time must be interpolated quadratically between output points in order to assure that the radial velocity of the subsatellite is zero. The velocity depends linearly on the error in release time and is therefore more critical than the position (and tension) which is a quadratic function of time near the minimum.

The next step in the analysis is to repeat the run adding the wire masses and using the reel maneuver parameters from the two mass runs. The presence of wire masses has various effects such as

shifting the center of gravity of the system (and altering the equilibrium tension as a result), introducing a delay in the propagation of tension signals between the Shuttle and subsatellite, and adding modelling of the longitudinal stress waves along the wire. For practical reasons it is not feasible to use large numbers of wire masses (such as 100) in the SKYHOOK program. Runs with up to 10 or 20 points can be done in a reasonable manner. The detailed results will depend on the number of mass points used in the model. The approach taken in the study is to use the difference in results with various numbers of masses as a measure of the uncertainty introduced by the discrete modelling of the physically continuous wire. In particular, the results with increasing number of mass points should not diverge in order to give confidence that the modelling of a particular problem is adequate. Wavelengths shorter than the spacing between mass points cannot be modelled. In the present study, the reel maneuver is of low frequency and has no sharp discontinuities which would introduce short wavelength effects.

In the multi-mass runs the first simulation is run without release of the payload to find the point of closest approach of the subsatellite. The tension plots are not useful for finding the release time because of the confusing effects of the longitudinal wire oscillations. A surprising result of the multi-mass run is that there seems to be almost no effect of propagation time on the response of the end mass. The time of closest approach of the subsatellite is only slightly later with the wire masses present than in the two-mass case which gives instant transmission of tension between the Shuttle and the subsatellite. The propagation time is short compared to the

period of the reel maneuver. One may conjecture that the time of closest approach may depend on the root sum square of the period of the reel maneuver and the propagation time rather than on the algebraic sum of the two. Unfortunately, the present study does not allow time to study this effect in detail and determine how the behavior depends on the period and propagation time. The tentative conclusion is that propagation time can be ignored as long as it is short compared to the period of the reel maneuver.

Two types of plots have been used to analyze the output of the computer runs. In one, tension in each wire segment is plotted as a function of time in order to see the magnitude of the tension variations and make sure that there is no loss of tension at any point along the wire. In the other, the radial vs. in-plane configuration of the wire is plotted at each output point in order to show the dynamics of the wire and the subsatellite. In a direct plot of the radial vs. in-plane coordinates, the dynamics of the reel maneuver does not show up because the motions are small compared to the length of the wire. In order to make the motions visible on a plot, the file of radial components has been processed to remove most of the constant part of the radial component. When the plot is scaled to fill the page, the motions in the radial and in-plane directions are amplified so that they can be seen easily. The processing of the radial components consists of the following. The SKYHOOK program produces a file of radial components  $R_I(t_j)$  where  $I$  is the mass index and  $t_j$  is the time index. A modified file  $R'$  is produced where  $R'$  is given by

$$R'_I(t_j) = r_I(t_j) - r_I(t_1) + (I-1) \Delta R$$

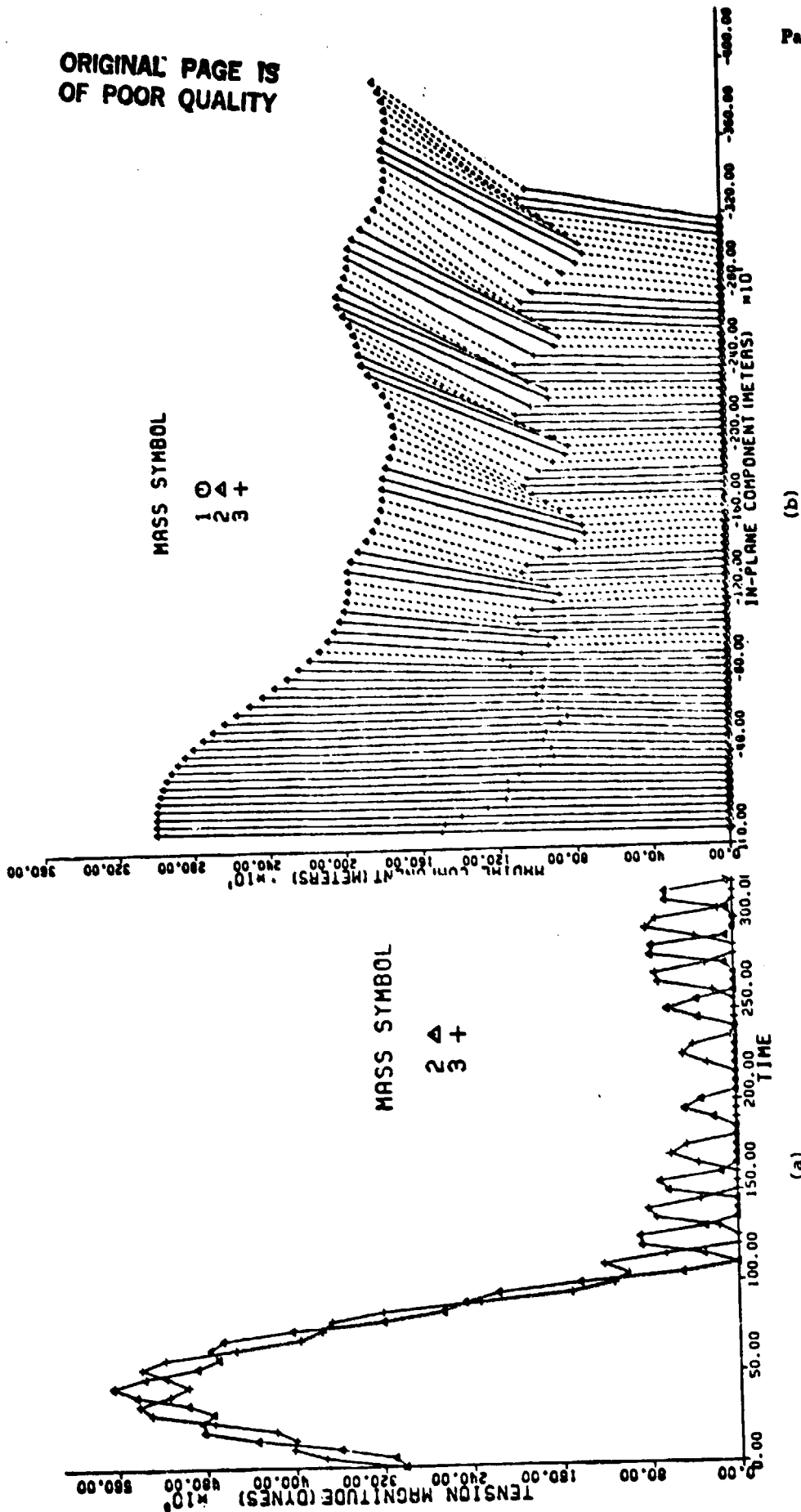


Figure 4-1. Payload release using a half-period sinusoid: three mass point model. Amplitude (length of tether reeled in during maneuver) = 933 meters, period = 104.7 seconds, release time = 141.8 seconds from start of maneuver. (a) Tension between mass points vs. time (b) radial vs. in-plane configuration: mass point spacing 1.5 km to show motions.

The constant  $\Delta R$  is chosen to be just large enough to prevent the plots for each mass from overlapping. In the case being studied the value of  $\Delta R$  is on the order of 1 km and the original spacing between mass points is on the order of 10 or more km depending on the number of mass points used to represent the wire.

#### 4.2 Results of Payload Release Study

This study has analyzed and compared four different cases of a payload release. For a 2mm tether, one reel maneuver using the equation  $-A \sin \omega t$  has been done and two runs using the equation  $A(\cos \omega t - 1)$  have been done for the half wave and full wave cases. Since the maximum tension during the reel maneuver was close to the break strength, another run was done with a 3mm wire and a full-wave reel maneuver. The principle effect of tether diameter is to alter the natural period for longitudinal oscillations of the mass at the end of the wire. This requires using a faster reel maneuver with a smaller amplitude. Otherwise, the basic approach is the same. For the 2mm tether with a full period reel maneuver simulations were done with 2, 3, 4, 5, 6, 7, 8, 9, and 10 masses in the model. For the 2mm half wave maneuver, 2 mass and 5 mass runs have been done. For the  $-A \sin \omega t$  reel maneuver, runs were done with 2 and 3 masses. For the 3mm full wave case, 2 mass and 10 mass runs were done.

All of these runs are done for an 80 km tether system deployed up with a released payload of 10 tons, a remaining payload of 0.5 ton and an Orbiter Mass of 100 tons.

In order to simulate the reel maneuver and payload release the SKYHOOK subroutines DIFFUN and TENSION have been modified. Subroutine DIFFUN reads the time for release of the payload and the mass remaining at the end of the tether after release. For times previous to release the subsatellite mass given on the normal input is used for mass number 2. After the release time the value for the remaining mass is used. Subroutine TENSION modifies the natural length of the wire segment next to the Shuttle according to the equation

$$l = l_0 - A \sin(\omega t + \phi) + A \sin(\phi)$$

where  $l_0$  is the natural length value in the normal input and the constants  $A$ ,  $\omega$ , and  $\phi$  are read along with  $t_f$  by subroutine TENSION. For times greater than  $t_f$  the value of  $l$  is computed with  $t = t_f$ .

As a starting point for the current analysis a simulation has been done with a reel maneuver given by  $-A \sin \omega t$  with  $\omega t$  going for a half cycle which corresponds to  $\phi=0$ . The amplitude  $A$  was determined from runs with a two mass model taking into account the effect of the shift in the center of mass on the equilibrium tension after payload release. A three mass simulation (one wire mass) was done using the parameters  $A = 933$  meters, period = 104.7 seconds and release time = 141.8 seconds. As in the previous study, there is some loss of tension as shown in Figure 4-1(a). The vertical axis is tension in dynes between each pair of mass points. The plotting symbol indicates the lower numbered mass of the pair. For the highest numbered mass, the tension is between that mass and the Shuttle which is mass number 1. Figure 4-1(b) shows the in-plane vs. radial configuration of the tether. The radial components have been altered by using a spacing of





Figure 4.2. Payload release using a half-period co-sinusoid: five mass point model. Amplitude = 533 meters, period = 209 seconds, release time = 230 seconds, reeling maneuver stop = 104.7 seconds. (a) Tension between mass points vs. time (b) radial vs. in-plane behavior: mass point spacing 2 km to show motions.

of 1.5 km between the curves for each mass point. This allows the plot scale to be expanded so that the motions in the vertical and horizontal direction are easily visible. The dotted lines indicate loss of tension in the tether segment.

In the next case, the phase angle  $\phi$  of the reel maneuver is set to  $-90^\circ$  so that the algorithm is basically a cosine function rather than a sine function. This eliminates the discontinuity in the first derivative at the start of the reel maneuver. In this run the reel maneuver goes for a half cycle so that the wire is pulled in but not let out again. The parameters for the run are  $A = 543$  meters, period = 209 seconds, and release time = 230 seconds. The reeling maneuver stops at 104.7 seconds. Figure 4-2(a) shows the tension as a function of time with 5 masses used in the model. There is no loss of tension and the tension variation after payload release is 27%. Figure 4-2(b) shows the radial vs. in-plane behavior. The curves are spaced 2 km apart in the vertical axis in order to obtain a convenient plot scale for making the motions easily visible.

The third case was run with a full-wave reel maneuver. The wire is pulled in and then let out again. The parameters of the run are  $A = 454$  meters, period = 139 seconds and release time = 159 seconds. Figure 4-3(a) shows the tension as a function of time and Figure 4-3(b) shows the in-plane vs. radial behavior with the curves separated by 1 km in the vertical axis. The tension variations after release are approximately 23%. Since the wire is a physically continuous system, which is being approximated by a set of discrete masses, it is important to provide an estimate of the uncertainty introduced by the modelling. For this reason, a set of runs with

ORIGINAL PAGE IS  
OF POOR QUALITY

Page 37

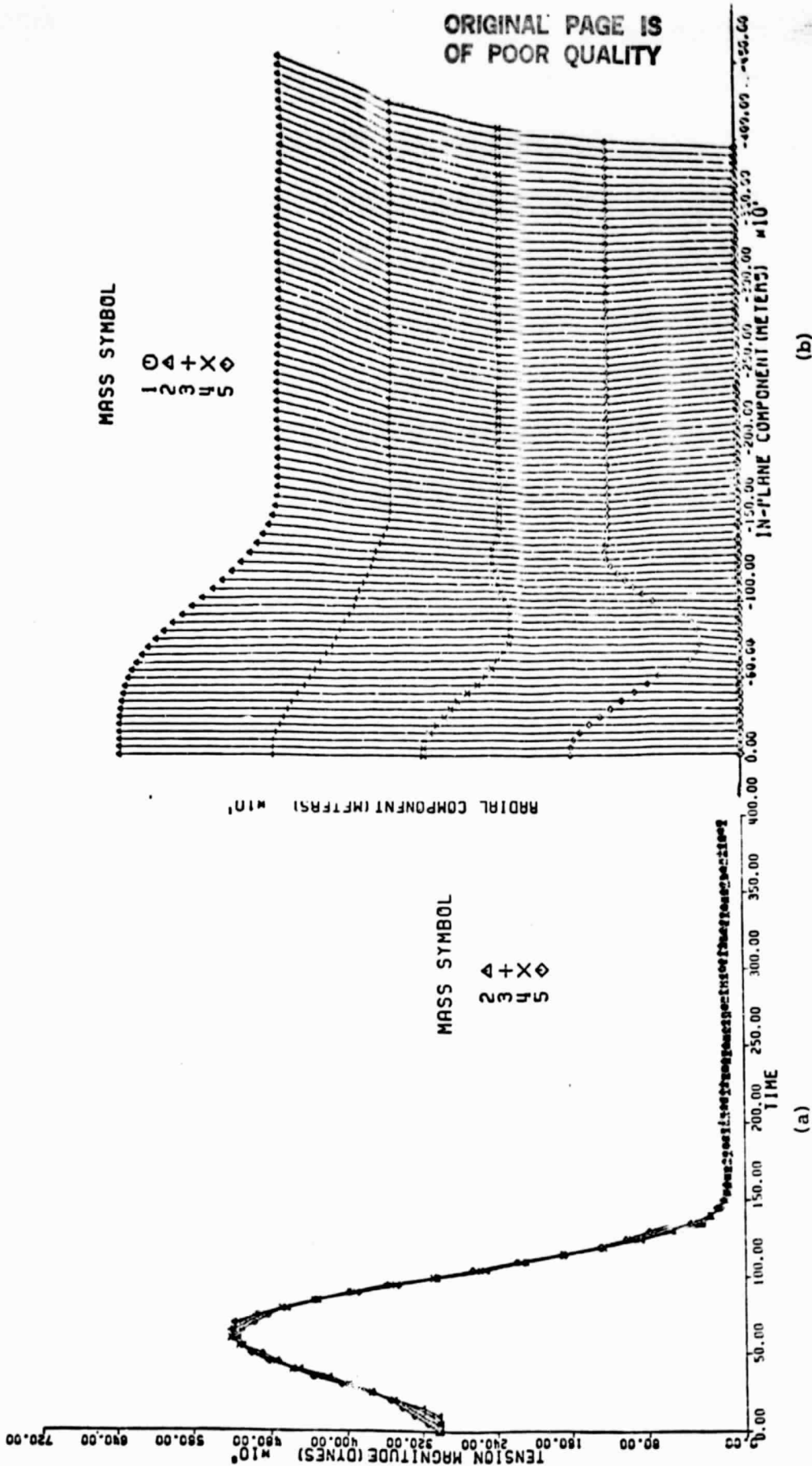
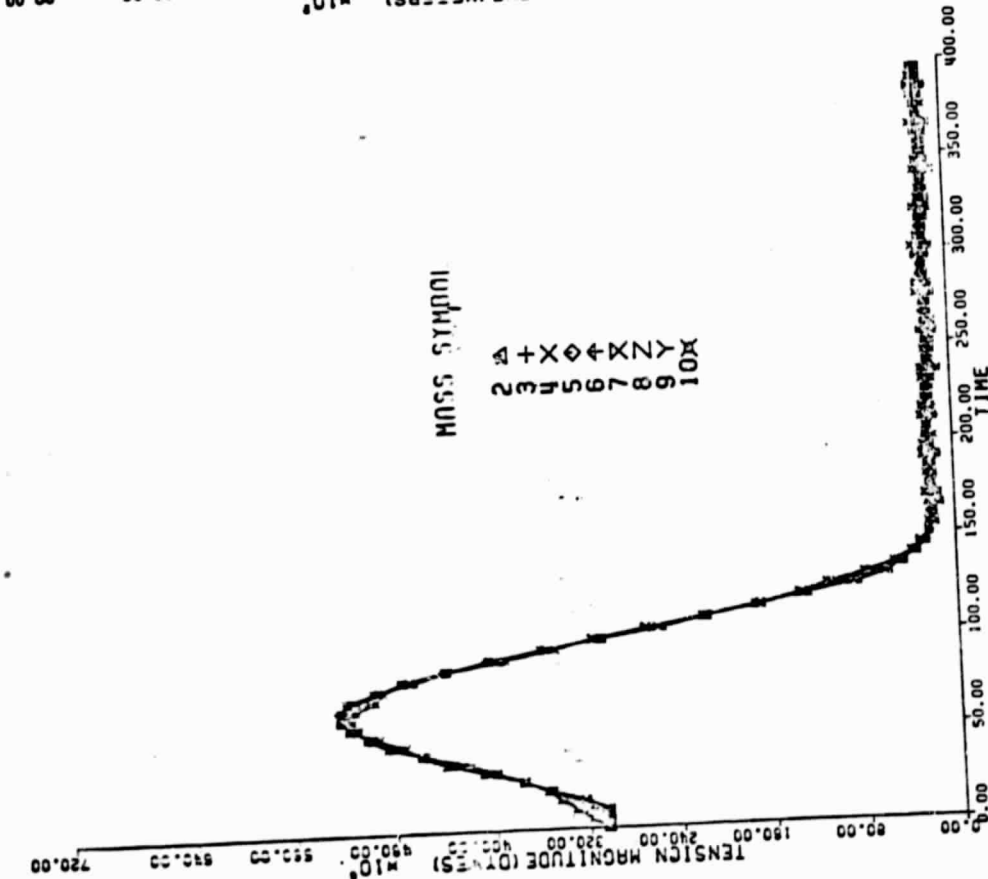


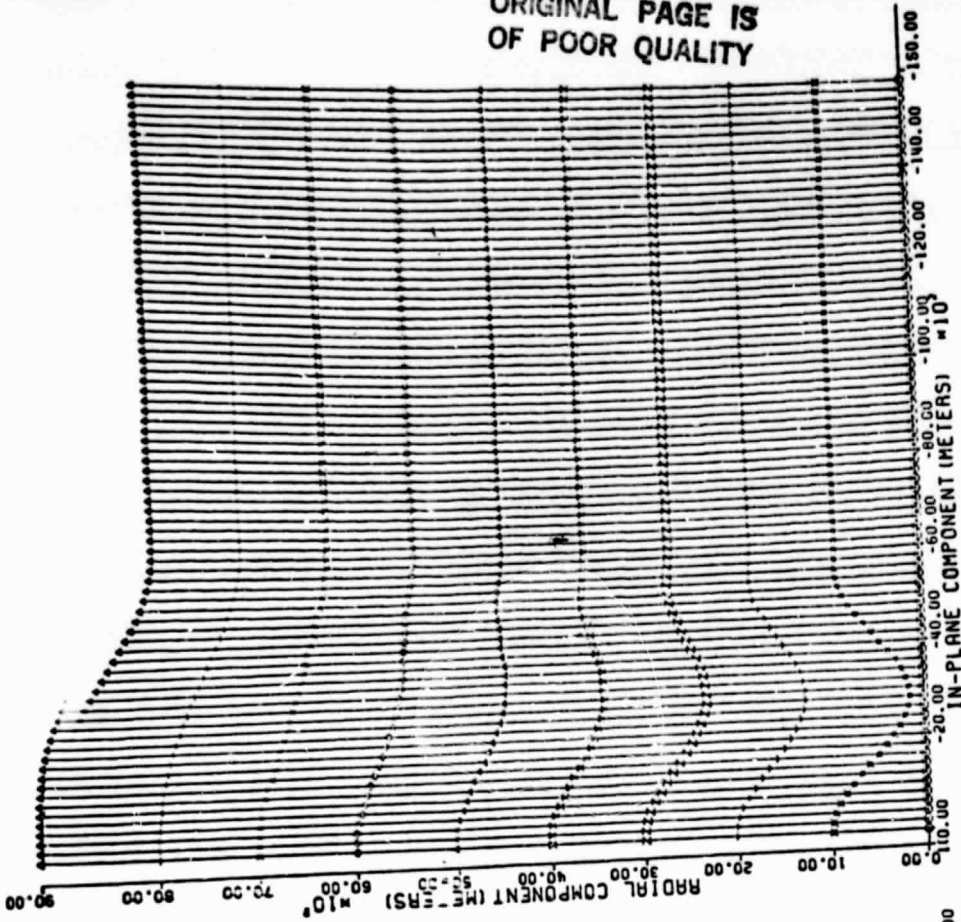
Figure 3. Payload release using a full-period co-sinusoid five mass point model. Amplitude = 454 meters, period = 139 seconds, release time = 159 seconds from start of maneuver. (a) Tension between mass points vs. time (b) radial vs. in-plane behavior: mass point spacing 1 km to show motions.

ORIGINAL PAGE IS  
OF POOR QUALITY

Page 38



(a)



(b)

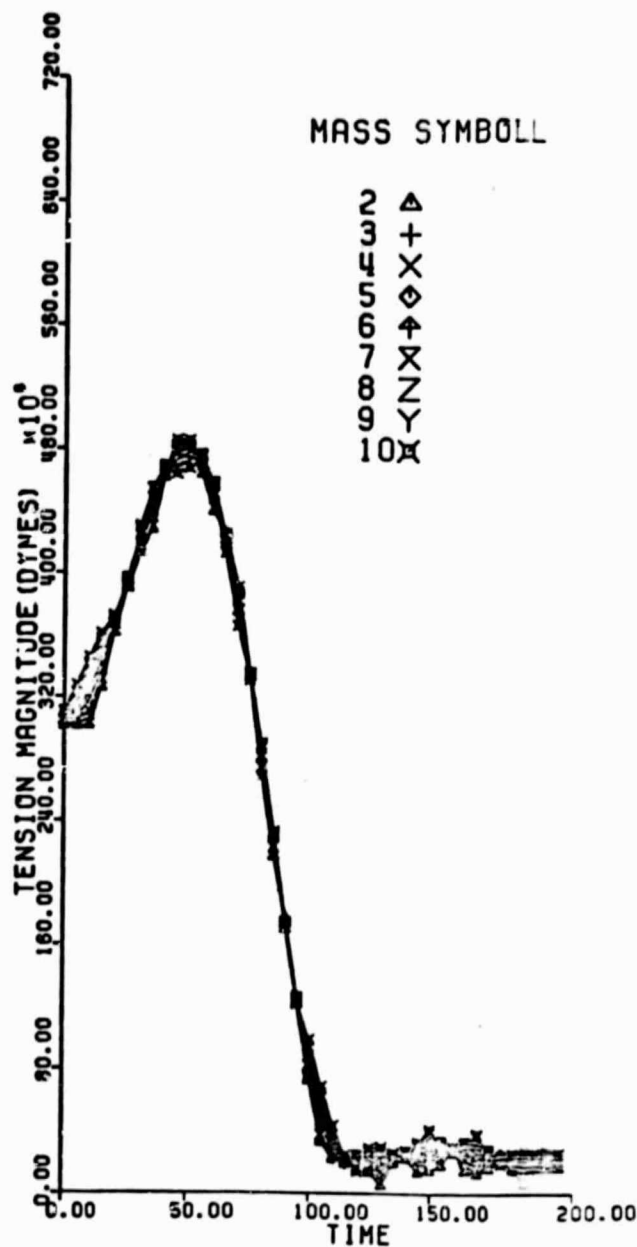
Figure 4-4. Payload release using a full-period co-sinusoid: ten mass point model. All parameters of run and figure same as Figure 4-3 (a) tension vs. time, (b) radial vs. in-plane behavior.

different numbers of masses in the model has been done for this particular case. The same parameters have been used for the reel maneuver in all cases. The table below shows the tension variation after payload release for each number of masses.

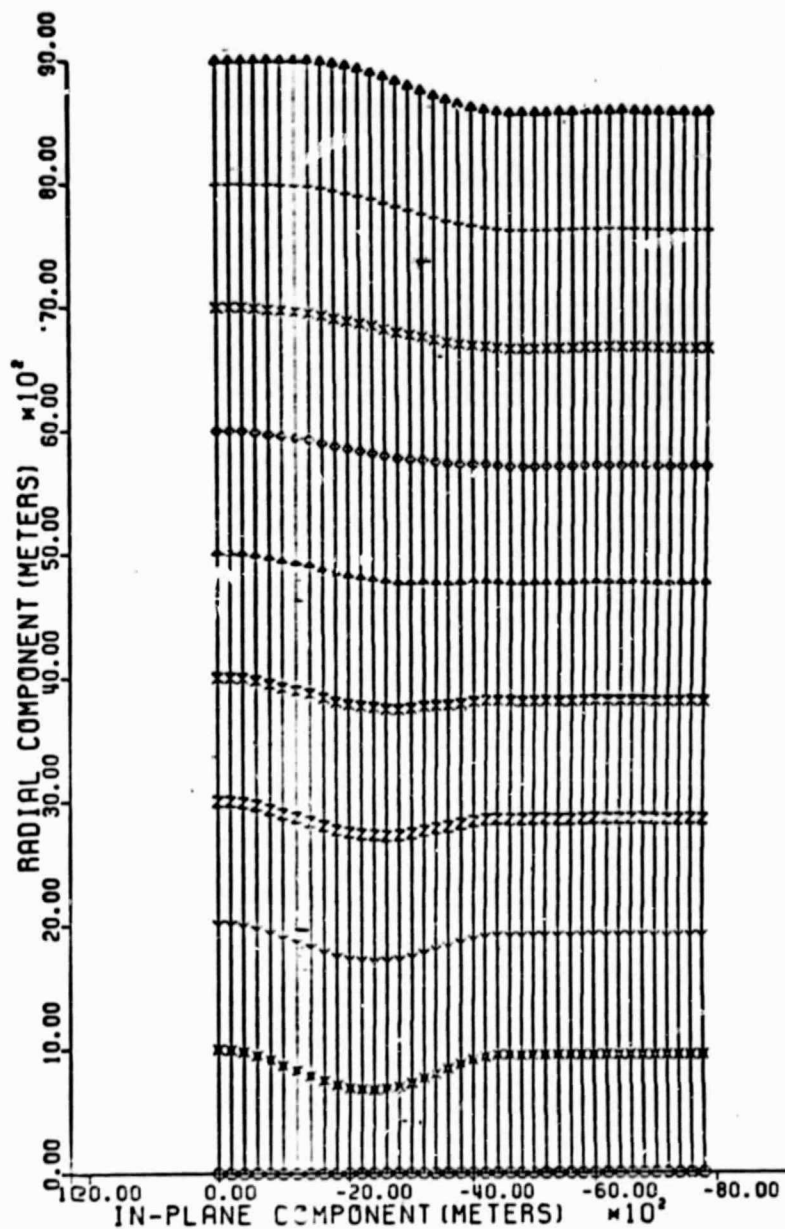
Number of Masses	% Tension Variation
2	1
3	81
4	51
5	23
6	50
7	57
8	55
10	55

The result for 2 masses is very low because wire excitations are not modelled. The highest tension variation was for 3 masses and the lowest for 5 masses. The value of 55% seems to be the best estimate and is fairly consistent for the larger numbers of masses, none of the runs show loss of tension in any of the wire segments. Figure 4-4 shows the results with 10 masses in the model. Part (a) is the tension vs. time and part (b) is the in-plane vs. radial configuration with 1 km spacing between the plots for each mass.

With a 2 mm diameter wire, the maximum tension induced by the reel maneuver is close to the break strength of the wire. Therefore, one final run was done with a 3 mm wire to provide results for a physically realistic case. The wire diameter affects the stiffness of the wire and therefore the natural frequency of the oscillations of the payload at the end. The period for the reel maneuver had to be reduced to keep it shorter than the response time of the end mass. Figure 4-5(a) shows the tension variation vs. time and Figure 4-5(b) shows the in-plane vs. radial with the curves separated by 9 km.



(a)



(b)

Figure 4-5. Payload release using a full period co-sinusoid: ten mass point model with 3mm diameter kevlar tether replacing 2mm diameter tether used in previous runs. Other parameters same as Figure 4-3 and 4-4. (a) Tension vs. time, (b) radial vs. in-plane behavior.

There is no loss of tension but the parameters are not optimized and there is an oscillation of the payload after release in addition to the wire oscillation. Unfortunately there was not sufficient time to find the cause of the problem and refine the parameters. One problem may be the fact that the tether mass is larger and the wire mass was not included in the center of mass calculations. The parameters used in the run are  $A = 176.6$  meters, period = 114.5 seconds, and release time = 117 seconds.

The major problem in the cases studied is the tension variations caused by longitudinal oscillations of the tether. The techniques developed in this study give satisfactory behavior for a case which is difficult because of the large ratio of the tension before release to the tension after release. The technique could be refined if necessary by developing an algorithm whereby the reel motor is used to damp longitudinal oscillations of the tether. Such an algorithm would have to be written as a function of the observables available at the reel motor such as tension and deployed tether length. The derivatives of these quantities could also be available by measuring the quantities at appropriate intervals. Such an algorithm would be of general usefulness in many tether operations.

The most unexpected feature of the simulations is the apparent absence of propagation delay in the response of the end mass. It would be interesting to study this effect in more detail to understand how it depends on the various time constants in the dynamics of the system such as the natural frequency of oscillation of the end mass, the period of the reel maneuver, and the speed of sound along the wire. A one-dimensional program exists which could be fairly easily

modified for use in such a study. By adding the gravity gradient force to this program, the propagation delay could be efficiently studied with the increased resolution provided by the larger number of mass that can be handled.

ORIGINAL PAGE IS  
OF POOR QUALITY



ORIGINAL PAGE IS  
OF POOR QUALITY

APPENDIX A

TETHERS FOR ORBITAL TRANSFER

AND SATELLITE SERVICING

Final Report on Subcontract SV2-52005

Submitted to

The Smithsonian Astrophysical Observatory

by

The Space Systems Laboratory  
Massachusetts Institute of Technology

Prepared by

M. . Martinez-Sanchez

Sarah A. Gavit

Mary L. Bowden

April 27, 1983

Table of Contents

	Page
<u>General Introduction</u>	1
1. <u>An Assessment of Shuttle-Based Tethers for Geosynchronous Transfer Assist</u>	
1.1 Introduction	1
1.2 Analysis	2
1.3 Results	9
1.4 Discussion of Results	10
References for Section 1	12
2. <u>Space-Based Tethers as Extension of the Space Transportation System for LEO-GEO Transfers</u>	
2.1 Introduction	16
2.2 Notation	17
2.3 Discussion of Results for Case (a) (Full Throw Weight)	18
2.4 Discussion of Results for Case (b) (Fixed OTV)	23
2.5 Summary and Conclusions	25
References for Section 2	
3. <u>Space-Based Tethers for Deep Space Launch Assist</u>	
3.1 Introduction	33
3.2 Analysis	34
3.3 Results	37
4. <u>Tether Servicing of Intermediate Altitude Satellites</u>	
4.1 Introduction	46
4.2 Orbital Precession Rates	47
4.3 Servicing of Sun Synchronous Satellites	51
4.4 Servicing of Science Platforms in Low Inclination Orbits	51
4.5 Rendezvous Dynamics	53
4.6 Orbital and Rendezvous Dynamics for the Case of an Elliptic Platform Orbit	60
4.7 Logistics of Servicing	64
References for Section 4	66

## General Introduction

This Report is a continuation and amplification of our previous Report entitled The Use of Tethers for Payload Orbital Transfer (March 22, 1982, Subcontract SV1-52006 from the SAO to MIT). The general topic is still the exploitation of very long, lightweight space tethers to supplement rocket propulsion in specific transfer missions. A preliminary examination is also made of a related application, namely, the retrieval of high-flying satellites from a space station for servicing.

Three orbital transfer applications are examined in depth in Sections 1, 2 and 3 of this Report. These are:

Section 1: In an effort to extract the maximum Shuttle payload capacity to Geostationary orbits, planned operations will involve very low altitude Shuttle flights, with reduced OMS fuel load, and, at least ideally, OTV vehicles designed to fill the allowable payload bay load capacity. The question posed in this section is whether the alternative of reducing the OTV size in favor of a permanent on-board tether facility for insertion assist can increase the GEO payload. For the specific case of LOX-LH<sub>2</sub> OTV's, the question is answered in the negative. The analysis shows that this is because some of the efficient OTV fuel is being replaced by the less efficient OMS fuel. Thus, either if the OMS fuel were replaced by LOX-LH<sub>2</sub> on the Shuttle, or if the OTV's used low I<sub>sp</sub> solid propellants, the results would have been different. The same thing would happen if the comparison were made (as in Section 2) to a fixed-size OTV which does not fill the throw weight limit.

Section 2: In our earlier work we had identified a possible system whereby a small automated space station houses the tether facility, which in this way

ORIGINAL PAGE IS  
OF POOR QUALITY

does not have to be flown up and down on board the Shuttle. The dynamics of the operations required to leave the facility in its initial orbit were also worked out. We reexamine here that concept under two different assumptions. First, if we limit the throw weight as in Section 1, the payload does increase relative to the on-board tether system, but is still slightly worse than that of an enlarged OTV that would replace all but the OMS fuel needed to reach minimum orbit. Second, if we assume a fixed-size OTV and compare its payload capacity to that of a system which uses the space-based tether as an auxiliary booster, there are definite gains due to the tethers (despite the extra Shuttle climb required).

Section 3: Here we examine again the Shuttle on-board tether, this time used with four different Centaur versions for an interplanetary mission, exemplified by the Jupiter Galileo probe. Payload increases of up to 400 Kg are found for all cases before the Shuttle perigee becomes too low, but the throw weight limitations restrict these gains to some 280 Kg for the small Centaur versions, and precludes the use of a tether facility in the larger ones. The 280 Kg boost makes one of the small Centaurs nearly capable of performing the Galileo launch.

Section 4 of this report examines briefly the use of long tethers from a permanent space station to retrieve and service satellites in higher orbits of the same inclination. The differential orbit precession rate due to the different altitudes is found to be too small to allow periodic revisits to Sun-synchronous satellites, but is quite adequate at inclinations up to  $\sim 45^\circ$ , including the important  $28.5^\circ$  case. Two possible schemes are examined: one involves a platform in circular orbit and exploiting the possibility of induced

ORIGINAL PAGE IS  
OF POOR QUALITY

tether librations to effect rendezvous between the tether-end teleoperator and the high satellite; the other scheme involves a platform in an elliptic orbit, with the tether sized to match teleoperator and satellite altitude and velocity. The docking phase is analyzed and some logistic considerations are advanced.

# 1. An Assessment of Shuttle-based Tethers for Geosynchronous Transfer Assist

## 1.1 Introduction

The possible use of long tethers carried on board the Space Shuttle as facilities for orbital transfer was briefly examined in Ref.1.1. It was recognized there that the mass penalty for the Shuttle-carried equipment associated with the deployment and retrieval of the tether made it difficult to obtain a net advantage from the scheme, except for high or very inclined orbits. The alternative of basing the tether in space was found superior, although issues such as orbit decay and Shuttle-tether rendezvous were not examined sufficiently.

Long range mission planning for the STS contemplates as much as 90% of all the Shuttle cargo as payload en route to Geosynchronous orbit. Given the relative inefficiency (both propulsive and structural) of the Shuttle as an orbit raiser, it makes sense to release the transfer stage at the minimum altitude consistent with orbit maintenance and avoidance of strong aerodynamic torques on the Shuttle. This is generally taken to mean a 90-100 nm orbit for the Shuttle. Shuttle operations below this altitude are probably unacceptable even for a fraction of an orbit, mostly because of attitude hold problems.

The question we wish to investigate in this report is whether the mass saving in propellant for the Orbital Transfer Vehicle (OTV) which can be obtained by releasing the OTV-payload combination from the end of an upwards deployed long tether is sufficient to compensate for the added on-board OMS fuel required for the Shuttle to fly to the correspondingly higher initial orbit, as well as for the mass of the tether system itself. In

ORIGINAL PAGE IS  
OF POOR QUALITY

this study, the payload capability of the Shuttle is considered limited by either (a) A maximum throw weight of 90,000 lb, or (b) A maximum OMS tankage capacity of 24,000 lb of propellant. Within these limits, the OTV itself is allowed to vary in size to reach one or the other operational boundary; the OTV structural fraction and specific impulse are taken to be those of an advanced LOX-LH<sub>2</sub> vehicle.

### 1.2. Analysis

Consider the fully loaded Shuttle initially placed in an elliptical orbit of perigee  $R_{po}$  and apogee  $R_{ao}$ . A tether of mass  $M_T$  and length  $L$  is released from a Shuttle-attached lower pallet, of mass  $M_{Lp}$ . The upper end of the tether carries an upper pallet of mass  $M_{up}$ , plus an OTV with its true payload  $M_{pay}$  attached ( $M_{OTV} + M_{pay} \equiv M_L$ ).

As the tether is deployed, the c.g. of the overall system stays (to 1st order) in the original orbit, while the Shuttle itself descends by

$$x_{cg} = \frac{M_L + M_{up} + \frac{1}{2} M_T}{M_{Tot2}} L \quad (1)$$

where 
$$M_{Tot2} = M_{sh} + M_T + M_L + M_{up} \quad (2)$$

and  $M_{sh}$  is the mass remaining in the Shuttle (including the lower tether pallet). In particular, at perigee passage, the Shuttle attitude (radius vector) is

$$R_{sh} = R_{po} (1 - \lambda) \quad (3)$$

with

$$\lambda = \frac{M_L + M_{up} + \frac{1}{2} M_T}{M_{Tot2}} \frac{L}{R_{po}} \quad (4)$$

This perigee passage is the most favorable location for payload release (maximum kinetic energy). The Shuttle has at this point a speed

$$V_{sh} = V_{po}(1 - \lambda), \text{ with } V_{po}^2 = \frac{\mu}{R_{po}} \frac{2R_{ao}}{R_{ao} + R_{po}}. \quad \text{After release, the Shuttle}$$

enters a new, lower elliptical orbit; assuming the initial eccentricity

$$\epsilon = \frac{R_{ao} - R_{po}}{R_{ao} + R_{po}} \quad (5)$$

is low enough, the Shuttle will reach its minimum altitude  $R_p$  at the opposite point in this new orbit. For the new system after payload release, the initial radius vector of its c.g. at the initial perigee is

$$R_{po}(1 - \lambda + \beta)$$

with

$$\beta = \frac{M_{up} + \frac{1}{2} M_T}{M_{Tot_2} - M_L} \frac{L}{R_{po}} \quad (6)$$

and its velocity is, correspondingly,  $V_{po}(1 - \lambda + \beta)$ . Let  $R'_p$  be the radius vector of this c.g. at its minimum altitude; then

$$\frac{\mu}{R_{po}} \frac{2R_{ao}}{R_{ao} + R_{po}} (1 - \lambda + \beta)^2 = \frac{\mu}{R_{po}(1 - \lambda + \beta)} \frac{2R'_p}{R'_p + R_{po}(1 - \lambda + \beta)} \quad (7)$$

Defining

$$\eta' = \frac{R_{po} - R'_p}{R'_p} \quad (8)$$

Equation (7) can be solved to 1st order to yield

$$\eta' = 7\lambda - 2\epsilon - 7\beta \quad (9)$$

This  $\eta'$  gives the fractional loss of altitude of the Shuttle from its initial perigee to its final one, after rewinding is complete. If rewinding is slow, there will be even lower perigee passages; in particular,



If no rewinding is done for the first half orbit after release, the lowest Shuttle altitude will be  $R_p$ , given by

$$\eta = \frac{R_{po} - R_p}{R_p} = 7\lambda - 2\epsilon - 6\beta \quad (10)$$

Whether  $R'_p$  (Eq.(9)) or  $R_p$  (Eq.(10)) is to be identified with the minimum altitude of 100 nm depends on a more detailed mission study.

We use here the slightly less restrictive choice of  $R'_p$ .

The next task is to evaluate the amount of OMS fuel needed for the Shuttle to perform the different portions of the mission. Let  $I_{sp1}$  be the specific impulse of the OMS engines (313 sec. in the present configuration), and let  $\Delta V$  be one of the several velocity increments involved (injection into the nominal 100 nm orbit, transfer to the initial elliptical orbit, reserve and maneuvering, and deorbiting). Then we define for each of them

$$\mu = 1 - e^{-\frac{\Delta V}{gI_{sp1}}} \approx \frac{\Delta V}{gI_{sp1}} \quad (11)$$

and find, to first order, that the total OMS fuel consumption is

$$M_{OMS} = (M_s + M_{Ts})(\mu_{inj} + \mu_{tr} + \mu_{r.m.} + \mu_{deorb.}) + \\ + M_L (\mu_{inj} + \mu_{tr} + \mu_{r.m.}) \quad (12)$$

where  $M_s$  is the empty Orbiter mass and  $M_{Ts}$  is the mass of the complete tether system.

For flights to high enough orbits, this  $M_{OMS}$  may come to equal the on-board tank capacity, assumed to be 24,000 lb., and thus it would constitute one operational boundary limiting payload. Otherwise, the maximum throw weight, defined here as

$$M_{throw} = M_{OMS} + M_L + M_{Ts} \quad (13)$$

is limited by structural considerations to 90,000 lbs, and this constitutes the operational boundary for low orbits.

The velocity increments themselves are evaluated as follows: first,  $\Delta V_{inj}$  is directly fixed at 30.5 m/sec (injection into a 100 nm, 23° orbit), and  $\Delta V_{r.m.}$  is fixed at 62 m/sec. Next the  $\Delta V$  for transfer to a  $(R_{po}, R_{ao})$  orbit, starting at  $R_p = 100$  nm is easily calculated as the sum of a perigee and an apogee impulse, where the terms perigee and apogee refer here to the transfer orbit itself; insertion is made at the lowest point ( $R_{po}$ ) of the destination orbit. The result is

$$\Delta V_{tr} = \Delta V_{tr1} + \Delta V_{tr2} = v_{cp} \frac{\eta'}{4} + v_{cp} \left( \frac{\epsilon}{2} + \frac{\eta'}{4} \right) = v_{cp} \frac{\epsilon + \eta'}{2} \quad (14)$$

where  $\epsilon$  is given by Eq. (5),  $\eta'$  by Eq. (8) and  $v_{cp} = \sqrt{\mu/R_p}$  is the parking orbit velocity.

The deorbiting maneuver is assumed to start from the eventual Orbiter apogee, (Eq.8), since a direct calculation shows this to be the location requiring least  $\Delta V_{deorb.}$ . The  $\Delta V$  is calculated as the impulse that will place the Orbiter into an elliptic orbit

just grazing the ground. A simple calculation yields, to first order,

$$\Delta V_{dceorb.} = v_{cp} \frac{\alpha}{4} \quad (15)$$

where  $\alpha$  is the ratio of minimum altitude to Earth radius:

$$\frac{R_{cp}}{R_E} = 1 + \alpha \quad (16)$$

The advantage of the use of tethers is, of course, the reduction of the propulsion requirements for the main LEO-GEO transfer; this reduction comes about because the payload starts out from

$$R_{LO} = R_{po}(1 + \lambda_L) \quad ; \quad \lambda_L = \frac{M_{SH} + \frac{1}{2} M_T}{M_{TOT2}} \quad (17)$$

with velocity

$$V_{LO} = V_{po}(1 + \lambda_L) = \sqrt{\frac{\mu}{R_p}(1+\epsilon)} (1 + \lambda_L) \quad (18)$$

Denoting by  $\rho$  the ratio of Geosynchronous to Low Earth radii

$$\rho = \frac{R_{GEO}}{R_{po}} \quad (19)$$

we can calculate the total  $\Delta V$  required (to be supplied by the OTV propulsion system) as the sum of a perigee and apogee impulse.

$$\Delta V_p = v_{cp} \sqrt{\frac{1}{1+\eta}} \left[ \sqrt{\frac{2\epsilon}{(1+\lambda_L)(1+\lambda_L+\rho)}} - (1+\lambda_L)\sqrt{1+\epsilon} \right] \quad (20)$$

$$\Delta V_a = v_{cp} \sqrt{\frac{1}{(1+\eta)\rho}} \left[ 1 - \sqrt{\frac{2(1+\lambda_L)}{1+\lambda_L+\rho}} \right] \quad (21)$$

ORIGINAL PAGE IS  
OF POOR QUALITY

In terms of this total  $\Delta V$  and of the OTV fuel load  $M_{P_2}$  and structural mass  $M_{OTV}$ , the payload delivered to GEO is

$$M_{\text{pay}} = \frac{M_{P_2}}{e^{\frac{\Delta V/g}{I_{sp2}} - 1}} - M_{OTV} \quad (22)$$

where  $I_{sp2}$  is the specific impulse of the orbital transfer vehicle.

The approach taken in this study was to allow the OTV/<sup>size</sup> to be dictated by the operational envelopes of the Orbiter (throw weight or OMS tankage). Thus, only the structural ratio and the specific impulse were prescribed, with the assumption that an optimized vehicle design could be made to fit the available total weight. The ratio adopted was that of the proposed Wide-Body Centaur.

$$\frac{M_{P_2}}{M_{OTV}} = \frac{44,146 \text{ lb}}{6,467 \text{ lb}} = 6.826$$

An important element in the present calculation is the mass model for the tether (of length  $L$ ) and associated elements. The tether itself is dimensioned using equations derived in Ref. 1.1.

$$M_T = (M_{up} + M_L) \frac{2\gamma^2}{1+\gamma} e^{\left(\frac{\gamma}{1+\gamma}\right)^2} \quad (23)$$

where

$$\gamma = \frac{L}{R_p} \sqrt{\frac{3}{2} \frac{\mu_0}{\sigma R_p}} \quad (24)$$

$$\gamma = \frac{M_{up} + M_L}{M_{SH}} \quad (25)$$

and where  $\sigma$  and  $\rho$  are the working stress and the density of the tether material, respectively. We assumed the material to be Kevlar-49, with

$$\sigma_{\text{break}} = 1.4 \times 10^9 \text{ N/m}^2 \text{ (long fiber)}$$

and

$$\rho = 1400 \text{ Kg/m}^3$$

A variable safety factor SF (nominal value = 2.5) was incorporated in the calculations.

The upper and lower pallet masses were assumed to vary with tether mass according to the schedule shown in Figs. 1.1a and 1.1b.

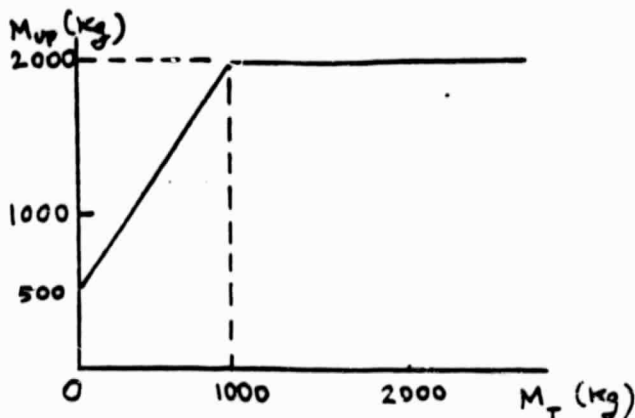


FIG 1.1a

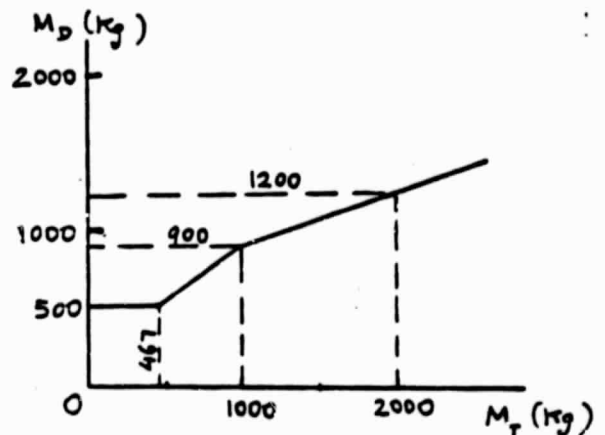


FIG 1.1b

These pallet masses were derived from simple scaling considerations, with no specific design worked out. The minimum weight of the pallet was made consistent with that of the small pallet designed in Ref. 1.2. Within reasonable limits (factors of 1.5 up and down), the precise choice of  $M_{up}$  and  $M_D$  did not affect the main conclusions of this study.

### 1.3 Results

A computer program was written to calculate the payload capability of a Shuttle-tether system using the equations described in Section 1.2. The inputs are tether length, minimum Shuttle altitude, eccentricity of the initial orbit and whether throw weight or fuel tankage limits payload.

For the case where throw weight is the limiting factor, and for circular initial orbit, Fig. 1.2 summarizes the variations of the principal masses involved with tether length. The main result is that the payload mass (MPA) continuously decreases with tether length. This negative result can be traced to two main reasons: (a) For short tethers (below ~ 1100 Km), where the mass of the tether itself (MT) and of the overall tether system (MTS) is still moderate, the increase of the OMS fuel mass required to acquire the initial higher Shuttle orbit is the dominant factor. (b) For longer tethers, the tether and tether system masses increase at least quadratically, and further reduce payload capability, despite a gradual levelling of the OMS fuel curve. Of course, the tether does reduce the fuel (and, correspondingly, the structure) needed for the transfer vehicle (MP2), and this by a substantial amount. Thus, if an OTV is not available that would actually fill the allowable throw weight, the use of tethers may still be a viable alternative to the construction of a larger OTTV.

The effect of starting from an initially eccentric orbit (payload release at perigee) is shown in Fig. 1.3, for a tether length of 1000 Km (similar trends apply at other lengths). Clearly, no advantages accrue from eccentricity, essentially because of the extra OMS fuel needed for the Shuttle to reach that initial eccentric orbit.

The underlying reason for the increased OMS fuel requirements associated with the use of tethers is illustrated in Fig. 1.4 (for circular orbits). Here we can see the additional Orbiter altitude required of the initial orbit over and above the minimum of 100 nm, versus the tether length. For short tethers, this amounts to about 1.8 Km per tether Km. This rate is gradually reduced for longer tethers, as the mass at the end of the tether (mostly OTV fuel) decreases and that on the Orbiter increases correspondingly; however, even for a 150 Km tether, an additional initial altitude of 175 Km is required.

Results for the case where the on-board OMS fuel is performance-limiting are similarly negative. This limitation arises, in the present context, for very long tethers, where the Shuttle is forced into a high initial orbit; we have already seen that for such long tethers, OMS fuel is no longer the dominant factor, this role having been taken by the tether system mass itself.

#### 1.4 Discussion of Results

In summary, we can see from the preceding results that replacing OTV fuel by an equivalent mass of tether facility always incurs some (although not much) performance loss. The emphasis is on the word "replacing"; basically, the tether imparts to the transfer vehicle a part of the momentum of the Shuttle itself, in an amount equal to that lost by the Shuttle as it goes from the release orbit to the minimum perigee orbit. This momentum was acquired by firing the OMS on-board engines, with a specific impulse of only 313 sec. Because of the restriction we imposed that the full throw weight be always utilized, this extra OMS fuel displaces a similar amount of OTV fuel, which has a higher specific impulse in our examples, and the result is a net loss.

From the preceding discussion several avenues can be seen that can lead to an advantageous use of an on-board tether facility:

- (a) Extension of Main Engine LOX-LH<sub>2</sub> burn to reach a high parking orbit.

This would displace the inefficient OMS fuel from its role as orbit-raiser.

- (b) Combination of tether facility with lower specific impulse OTV vehicles, such as the IVS or the PAM family. These have even lower  $I_{sp}$  than the on-board N<sub>2</sub>O<sub>4</sub> - A50 engines, and the tether would then prove an advantage.

- (c) If a given OTV is to be used and there is still a load margin before the throw weight limit is reached, this margin could be exploited by using an on-board tether, as an alternative to developing a larger OTV.



References

- 1.1 "The Use of Tethers for Payload Orbital Transfer." Final Report on Subcontract SV1-52006 to the Smithsonian Astrophysical Observatory, from the M.I.T. Space Systems Lab. By M. Martinez-Sanchez, March 1982.
- 1.2 Ch. C. Rupp and J.H. Laue, "Shuttle Tethered Satellite System," Paper AAS-78-048.

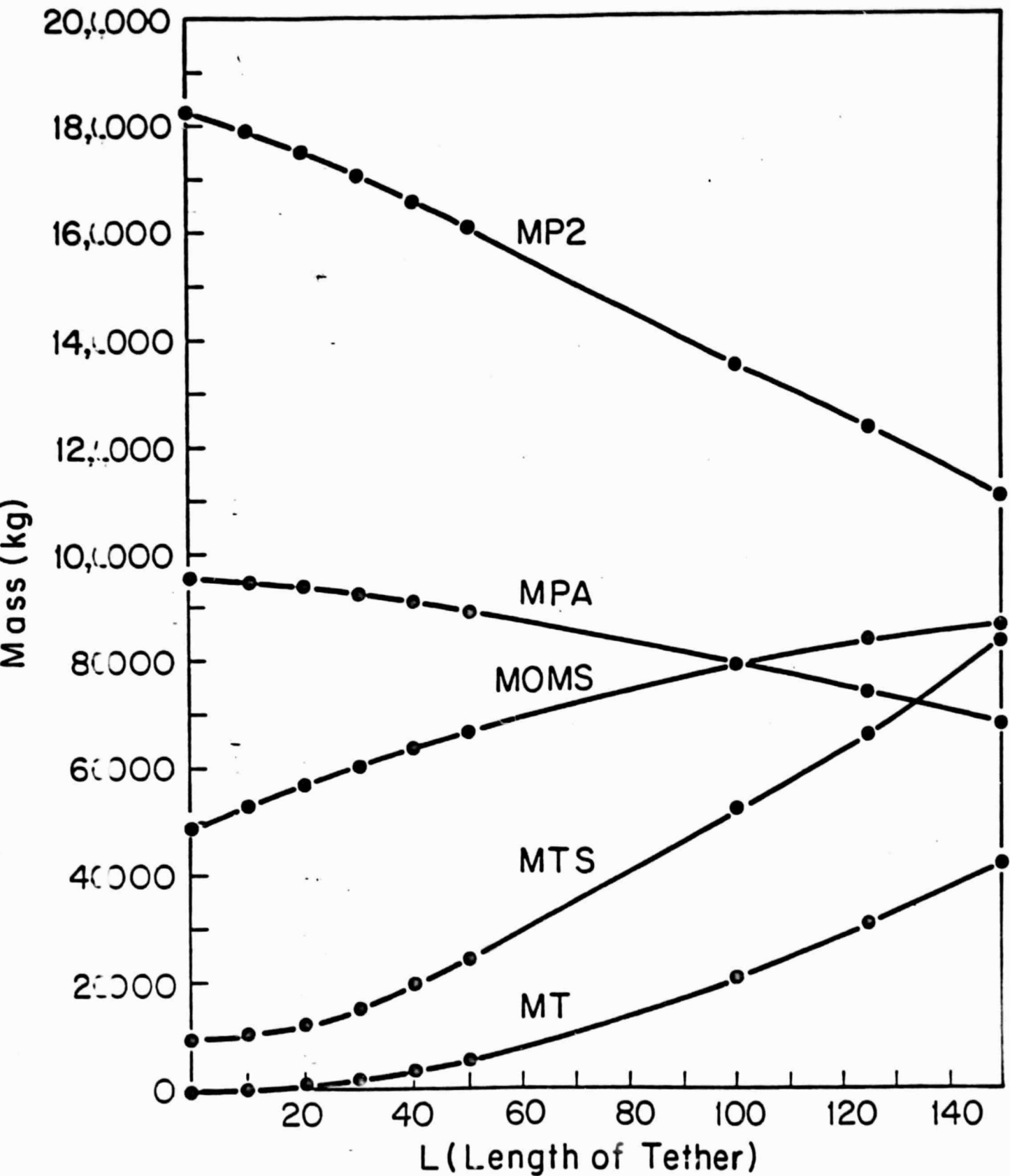
ORIGINAL PAGE IS  
OF POOR QUALITY

Fig. 1.2 Important Mass Parameters vs. Length of Tether  
at Zero Eccentricity

ORIGINAL PAGE IS  
OF POOR QUALITY

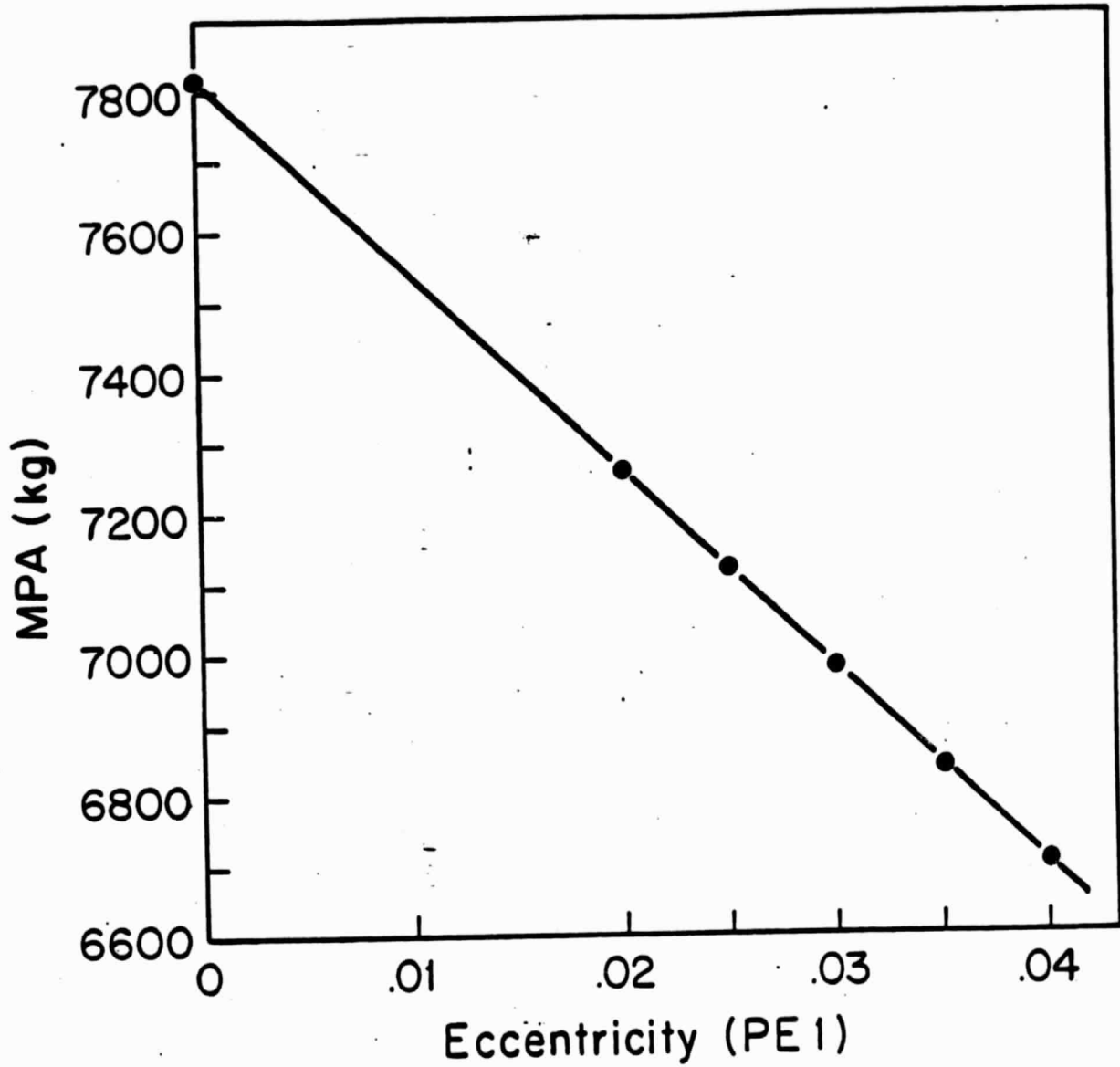


Fig. 1.3 Shuttle Payload vs. Eccentricity  
at Tether Length = 100 Km

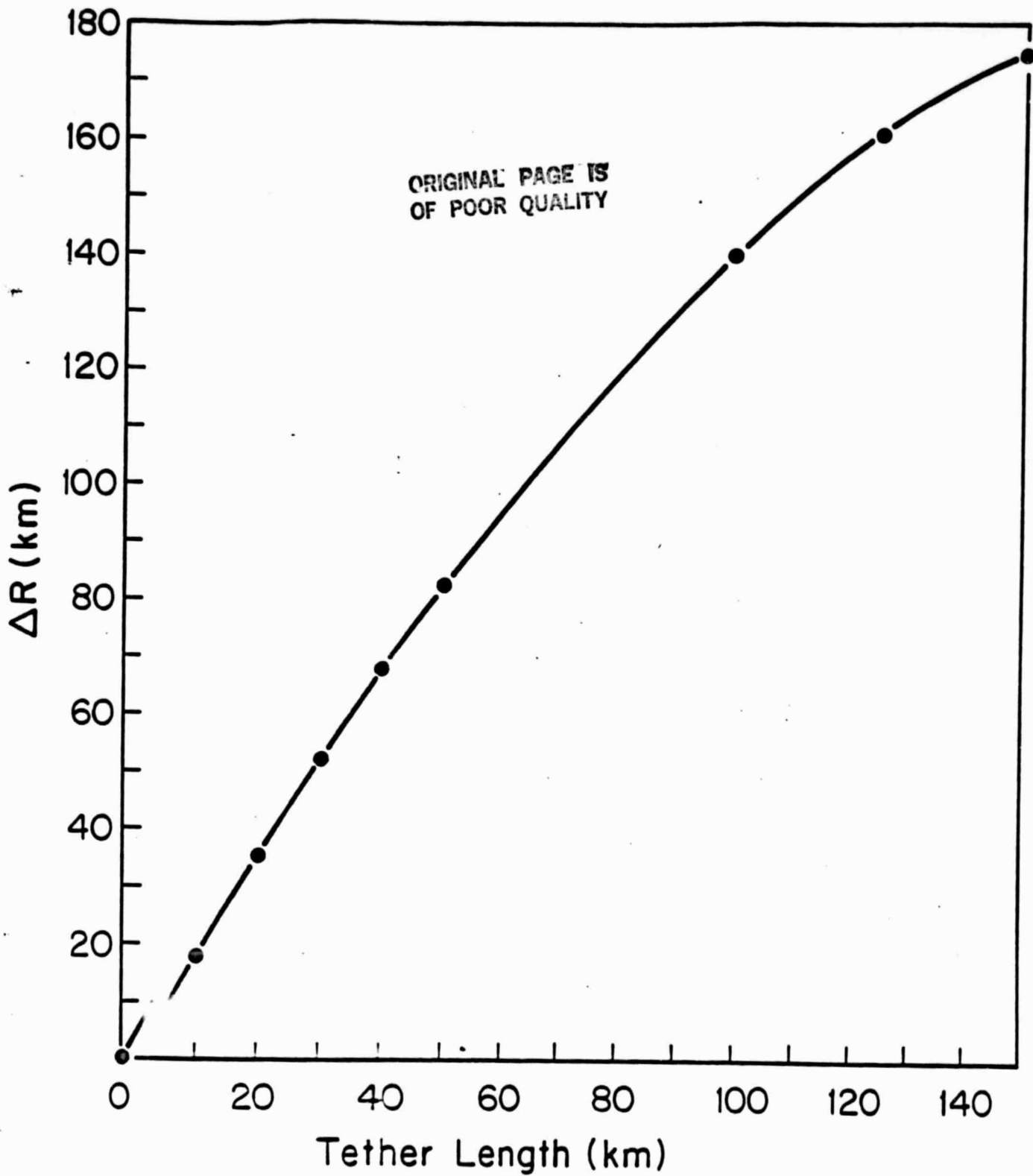


Fig. 1.4 Required Change in Altitude (perigee)  
for Given Tether Length

## 2. Space-based Tethers as Extensions of the Space Transportation System for LEO-GEO Transfers

### 2.1 Introduction.

In Section 1, we examined in some depth the possibility of using a tether system on board the Space Shuttle as an aid in launching satellites into GEO-bound transfer orbits. It was assumed that the maximum throw-weight of the Orbiter was always utilized (including the OTV with its payload, the tether system and the on-board OMS fuel), and that the Shuttle delivered the payload using the on-board tether to as low an orbit as possible, without itself being forced to altitudes below 100 n.m. The full tether system (lower and upper pallets plus rewound tether) was returned to Earth after each mission. It was concluded on the basis of the calculations performed that this system could not deliver as much payload to GEO as the baseline system without tethers. The difficulty was traced to two main points: (a) For short tethers (below some 100 km), the dominant effect was the extra OMS fuel required for the Shuttle to achieve the required delivery height; since the throw weight was limited, this extra was reflected in a smaller payload. (b) For long tethers, the need to carry a massive tether system to and from orbit became dominant and, again, detracted from payload.

In this section we investigate the effects of removing one of these constraints, namely, the transportation of the tether system. This is accomplished by leaving this system in orbit, in a manner described and analyzed in Ref. 2.1. We perform the corresponding calculations for two limiting cases: (a) Full throw weight utilization (similar to our study for the Shuttle-based tether system). This implies a different OTV size for each choice of tether

length or other parameters; as such, it represents a maximum payload envelope, and is appropriate for system definition studies.

(b) Fixed Orbital Transfer Vehicle, maximum OMS fuel use. This case corresponds more closely to a practical situation where a particular OTV, such as some modified Centaur, is available, and the Shuttle cargo capacity is not completely used up by this OTV plus its payload. Here the tether can be viewed as a boost to the OTV, rather than a partial substitute.

2.2 Notation. The following notation is used in the analysis:

$L$	tether length (full)
$\ell$	tether length (partially rewound)
$x$	for a deployed tether, distance from its lower end to the c.g. of the tether-platform-payload system
$x'$	same, but to the c.g. of the tether system alone
$\tilde{x}'$	same as $x'$ , but after partial rewinding
$R_{LEO}, h_{LEO}$	radius and altitude to the initial (and final) orbit of the tether system
$R_{MIN}, h_{MIN}$	Minimum radius and altitude for the Orbiter (set at 100 n.m.). For case (a), this is also the altitude from which the Orbiter will reenter.
$\Delta V_{inj,rm}$	Shuttle velocity increments from MECO to attain parking orbit at $h_{MIN}$ , and for reserve and maneuvering. Taken as 92.5 m/sec.
$\Delta V_{tr}$	$\Delta V$ for transfer from parking orbit to tether system orbit, at $h_{LEO}$
$\Delta V_{deorb}$	Deorbiting $\Delta V$ for Shuttle
$\mu = 1 - e^{-\Delta V/c_{OMS}} \approx \Delta V/c_{OMS}$	, where $c_{OMS} = g(I_{sp})_{OMS}$ is the effective jet speed for the OMS rockets (taken as 9.8x313 m/sec)
$M_{OMS}$	Mass of OMS fuel needed on the Shuttle. Limited to 24,000 lb
$M_L$	Loaded OTV mass (including payload)
$M_{throw}$	Shuttle throw weight, limited to 90,000 lb. Since the tether system is left in orbit, we take $M_{throw} = M_{OMS} + M_L$

ORIGINAL PAGE IS  
OF POOR QUALITY

$M_T$  tether mass

$M_{up}, M_{Lp}$  masses of the upper and lower pallets at the tether ends.

$M_{up}$  taken to be 2000 Kg.  $M_{Lp}$  variable.

$M_{TS} = M_T + M_{up} + M_{Lp}$  tether system mass

$\Delta V_1, \Delta V_2, \Delta V$  perigee, apogee and total velocity increments supplied by OTV. No change of plane assumed

$M_{p2}, M_{OTV,s}, M_{pay}$  - OTV propellant, OTV structural mass and carried payload (to Geosynchronous orbit).

(SF) - safety factor for tether material. Nominal value = 3.

$\sigma$  - break strength of tether. Taken as  $1.4 \times 10^9$  N/m<sup>2</sup>

$\rho$  - density of tether material taken as 1440 Kg/m<sup>3</sup>

### 2.3. Discussion and Results for Case (a) (Full Throw Weight)

The sequence of events here is:

- (a) The tether system has been orbited to the appropriate altitude (corresponding, as will be seen, to a given tether length, and other system parameters).
- (b) The Shuttle goes from MECO to parking orbit, then to the tether orbit, and docks with the Lower Pallet.
- (c) Tether unwinds with the OTV at its end. After stabilization, OTV is released.
- (d) Partial rewinding of tether (to length  $l < L$ ) from the Shuttle, then the Shuttle detaches. Rewinding completed from Lower Pallet. Tether system is back in original orbit.
- (e) Shuttle, after detaching, is in elliptic orbit with perigee at  $h_{MIN}$ . Deorbiting burn applied at one apogee passage.

The size of the Orbital Transfer Vehicle is here assumed variable, and is always selected such as to fully utilize the available throw weight capacity:

$$M_{OMS} + M_L = (M_{throw})_{MAX} \quad (1)$$

The payload, fuel and structural masses making up  $M_L$  are then apportioned according to the required  $\Delta V$  for transfer to GEO and the prescribed structure/fuel ratio for the OTV. The  $\Delta V$  itself depends on the altitude and speed of the payload at the instant of release from the tether; thus all of the variables interact with each other and an iterative calculation is required. The algorithm used was as follows:

(1) Select inputs:  $(M_{throw})_{MAX}$ ,  $M_{Shuttle, empty}$ ,  $\Delta V_{inj, rm}$ ,  $c_{OMS}$ ,  $c_{OTV}$ ,  $M_{OTV, s}/M_{p2}$ ,  $M_{up}$ ,  $L$

(2) Guess  $x/L$ ,  $\frac{x' - \tilde{x}'}{L}$

(3)  $R_{LEO} = R_{min} + 7 L \left( \frac{x}{L} - \frac{x' - \tilde{x}'}{L} \right)$  (from Ref. 1)

(4)  $f = 1 + \frac{L}{R_{LEO}} \left( 1 - \frac{x}{L} \right)$ ;  $\rho = \frac{R_{GEO}}{R_{LEO}}$ ;  $\eta = 1 - \frac{R_{min}}{R_{LEO}}$ ;  $v_{cp} = \sqrt{\frac{\mu_e}{R_{min}}}$

$$\Delta V_1 = \frac{v_{cp}}{\sqrt{1+\eta}} \left( \sqrt{\frac{2\rho}{f(f+\rho)}} - f \right); \quad \Delta V_2 = \frac{v_{cp}}{\sqrt{1+\eta}} \left( 1 - \sqrt{\frac{2f}{f+\rho}} \right)$$

$$\Delta V = \Delta V_1 + \Delta V_2$$

(from Ref. 2.2)

(5)  $\mu_{inj, rm} = \frac{\Delta V_{inj, rm}}{c_{OMS}}$ ;  $\mu_{tr} = \frac{v_{cp}}{c_{OMS}} \frac{\eta}{2}$ ;  $\mu_{deorb} = \frac{v_{cp}}{c_{OMS}} \frac{1}{4} \frac{h_{min}}{R_E}$



$$(6) \quad M_L = \frac{M_{\text{throw}} - M_{\text{SH,E}}(\mu_{\text{inj,rm}} + \mu_{\text{tr}} + \mu_{\text{deorb}})}{1 + \mu_{\text{inj,rm}} + \mu_{\text{Er}}}$$

$$(7) \quad M_{P_2} = M_L (1 - e^{-\Delta V/c_{\text{OTV}}}) \quad M_{\text{OTV,s}} = \left( \frac{M_{\text{OTV,s}}}{M_{P_2}} \right) M_{P_2}$$

$$M_{\text{pay}} = M_L - M_{P_2} - M_{\text{OTV,s}}$$

$$(8) \quad \gamma^2 = \frac{3}{2} \frac{\mu \rho L^2}{\sigma R_{\text{LEO}}^3} = 6.14 \times 10^8 \frac{(\text{SF}) L^2}{R_{\text{LEO}}^3} \quad v = \frac{M_{\text{up}} + M_L}{M_{\text{sh}}}$$

$$m_T = (M_{\text{up}} + M_L) \frac{2\gamma^2}{1+\gamma} e^{-\frac{\gamma^2}{(1+\gamma)^2}} \quad (\text{Ref. 4})$$

$$(9) \quad M_{\text{LP}} = 2000 + 1.5 M_T$$

$$(10) \quad M_{\text{TS}} = M_{\text{LP}} + M_T + M_{\text{up}} \quad ; \quad M_{\text{TOT}} = M_{\text{SH}} + M_{\text{ts}} + M_L$$

$$(11) \quad \frac{\ell}{L} = -\frac{M_{\text{up}}}{M_T} + \sqrt{\left( \frac{M_{\text{up}}}{M_T} \right)^2 + 2 \frac{M_L}{M_{\text{TOT}}} \frac{M_{\text{TS}}}{M_T} \frac{M_{\text{SH,E}} + M_{\text{LP}} + M_T/2}{M_{\text{SH,E}}}} \quad (\text{Ref. 2.1})$$

$$(12) \quad \frac{x}{L} = \frac{M_L + M_{\text{up}} + M_T/2}{M_{\text{TOT}}} \quad ; \quad \frac{x' - \tilde{x}'}{L} = \frac{1}{2} \frac{M_T(1-\ell/L)}{M_{\text{TOT}} - M_L} \quad (\text{Ref. 2.1})$$

$$(13) \quad \text{Compare to assumed values; iterate to convergence}$$

The results of these calculations are summarized in Figs. 2.1, 2.2 and 2.3.

Fixed parameters were

$$h_{\text{MIN}} = 182 \text{ Km} \quad (v_{\text{cp}} = 7793.9 \text{ m/sec})$$

$$M_{\text{up}} = 2000 \text{ Kg} \quad , \quad \text{SF} = 3$$

$$(M_{\text{throw}})_{\text{MAX}} = 90,000 \text{ lb} \quad , \quad M_{\text{SH,E}} = 80,000 \text{ Kg}$$

$$M_{P_2}/M_{\text{OTV,s}} = 6.826$$

$$I_{\text{OMS}} = 313 \text{ sec} \quad , \quad I_{\text{OTV}} = 460 \text{ sec}$$

The most important result in Fig. 2.1 is the fact that the payload mass  $M_{PAY}$  decreases with tether length  $L$ , although much less than was the case in the similar calculations for Shuttle-carried tether systems (Sec. 1). Increasing  $L$  does allow a reduction in both fuel and structural OTV masses (see Fig. 2.1), but the increase in required OMS Shuttle fuel is still enough to offset these gains. Also shown in Fig. 2.1 are the tether and tether system masses; this mass is not a penalty in this case, since it will stay in orbit. Depending on tether length, the mass of this "mini-space station" goes from 4000 to some 15000 Kg. It can also be seen that throughout the range investigated ( $L \leq 160$  Km), the assumed OMS tankage capacity of 24,000 lb. is not exceeded.

From a fundamental point of view, the result that the payload is reduced by the use of a tether could be anticipated. In Ref. 2.1 it was shown that, to first order, the amount of fuel used to recover the perturbed orbit of the tether reaction mass after payload release is the same as that saved by the payload propulsion system due to the tether boost if the two propulsion systems have equal specific impulses. Here we do not exactly restore the perturbed orbit, since the Shuttle eventually reenters from an elliptic orbit different than the initial, circular one. However, we can expect that the use of the low specific impulse OMS rockets to supply the required orbital boosts for the Shuttle will always be disadvantageous when compared to the capabilities of enlarged OTV engines, with their higher specific impulse. Once again, this points at the desirability of using high specific impulse electric propulsion for restoring the perturbed orbits, such as discussed in Ref. 2.4. Alternatively, tethers can be used as supplements to, rather than as substitutes for chemical propulsion stages (see Section 2.4 of this Report)

The underlying reason for the large OMS fuel increase is the need to fly the Shuttle to higher orbits than the minimum altitude orbit at  $h_{MIN}$ . This is illustrated in Fig.2.2, which shows the altitude required for the tether system - for each tether length.

As indicated in the discussion, the tether is partially rewound from the Shuttle before the latter detaches, in order to restore the tether system to its original orbit. Fig.2.3 shows the fraction  $l/L$  left for autonomous rewinding. It can be seen in Fig.2.3 that for lengths beyond some 123 Km, it becomes impossible to restore the initial tether orbit, unless some additional unwinding is done after tether release. This would probably be only a minor difficulty, however.

Some additional calculations were performed to learn about the sensitivity of these results to various parameter variations. A brief discussion is given of each of these.

(a) Assuming the OMS system could be made to operate on LOX-LH<sub>2</sub> fuel ( $I_{sp} = 460$  sec), just as the OTV itself, we find for tether lengths of 0 and 100 Km the following results:

L (Km)	0	100
$M_{pay}$ (Kg)	12,413	12,276

Thus, even with this favorable assumption there is a slight performance loss due to the tether. This must be ascribed to the incomplete restoration of the reaction mass to its initial state, i.e., the Shuttle actually takes away some extra momentum that could have gone to the payload.

(b) With  $I_{OMS}$  back at 313 sec, if the upper pallet mass is increased from 2000 to 4000 Kg, for  $L = 100$  Km, the payload is reduced from 11,340 Kg

to 11,304 Kg, while the fraction  $l/L$  decreases substantially (from 0.948 to 0.739).

(c) With  $M_{up}$  back at 2000 Kg, variations in the assumed tether safety factor have the following effects (for  $L = 100$  Km):

SF	2	3	4
$M_{pay}$ (Kg)	11,334	11,340	11,345
$M_T$ (Kg)	1,932	2,929	3,946
$h_{LEO}$ (Km)	383.8	383	382.3
$l/L$	0.877	0.948	0.995

Thus, curiously enough, heavier tethers ensure higher payload mass.

(d) A similar effect was found by arbitrarily increasing the lower pallet mass from  $2000 + 1.5 M_T$  to  $4000 + 1.5 M_T$ . This increased the payload from the base value of 11,340 Kg to 11,353 Kg. At the same time it required  $l/L = 1.068$  (up from 0.948).

#### 2.4 Discussion and Results for Case (b) (Fixed OTV)

Here the propellant and structural masses of the Orbital Transfer Vehicle were arbitrarily fixed at the values (corresponding to one version of the Centaur vehicle)

$$M_{p_2} = 10,870 \text{ Kg}$$

$$M_{OTV,s} = 3230 \text{ Kg}$$

Given this condition, the largest payload to GEO can be secured by using the full OMS fuel complement of the Shuttle, for any tether length (or without tether). This was therefore assumed for the calculations in this section. Correspondingly, the perigee altitude of the Shuttle after

releasing the tether is no longer constrained to be  $h_{MIN}$ , only to be above this level (at an altitude called  $h_{deorb}$ ). Also, the throw weight is in this case below its maximum value, corresponding to the notion of a partially loaded Shuttle.

The calculation procedure used in this case was as follows:

- (1) Select fixed parameters (as in Case (a), except that  $M_{OMS}$ ,  $M_{p2}$  and  $M_{OTV,s}$  are fixed, and  $M_{throw}$  is not)
- (2) Guess  $\frac{x}{L}$ ,  $\frac{x' - \tilde{x}'}{L}$  and  $h_{deorb}$ .
- (3)  $R_{LEO} = R_{deorb} + 7 L (\frac{x}{L} + \frac{x' - \tilde{x}'}{L})$
- (4) Calculate  $f$ ,  $\rho$ ,  $\eta$ ,  $\Delta V_1$ ,  $\Delta V_2$ ,  $\Delta V$ , as in case (a)
- (5)  $\mu_{inj,rm} = \frac{\Delta V_{inj,rm}}{c_{OMS}}$ ;  $\mu_{tr} = \frac{v_{cp}}{c_{OMS}} \frac{\eta}{2}$ ;  $\mu_{deorb} = \frac{v_{cp}}{c_{OMS}} \frac{h_{deorb}}{4 R_E}$
- (6)  $(M_L^{(1)}) = \frac{M_{p2}}{1 - e^{\Delta V/c_{OTV}}}$       (2)  $M_L^{(2)} = \frac{M_{OMS} - M_{SH,E} \mu_{deorb}}{\mu_{inj,rm} + \mu_{tr}} - M_{SH,E}$
- (7) Compare  $M_L^{(1)}$  to  $M_L^{(2)}$ . If not equal, select new  $h_{deorb}$ , iterate.
- (8)  $M_{pay} = M_L - M_{p2} - M_{OTV,s}$

Steps (9) and beyond are as in Case (a). Eventually a new set of values of  $\frac{x}{L}$ ,  $\frac{x' - \tilde{x}'}{L}$  is generated, which must agree with the initial guess. This is ensured by an outer iteration loop.

The results using  $M_{OMS} = 24,000$  lbs are presented in Figs. 2.4, 2.5 and 2.6. In Fig. 2.4 the essential result is the increase of  $M_{pay}$  with tether length.

This is as expected, since the tether system acts now as a supplementary booster over and above the fixed OTV. The increase amounts to a 12% per 100 Km of tether, and may make this a practical option for expanding the capabilities of an otherwise fixed Space Transportation System.

The other masses of interest are also displayed in Fig.2.4. As indicated, the sum of  $M_L$  and  $M_{OMS}$  never exceeds the maximum throw weight of 90,000 lb. Fig.2.5 shows the required orbital altitude for the tether system ( $h_{LEO}$ ) and the corresponding minimum perigee ( $h_{deorb}$ ) of the Shuttle. This latter altitude is always above the minimum of 183 Km. Also, the tether system altitude ranges from 425 to 489 Km, which is high enough to make drag effects negligible on the orbiting system.

The partial rewinding length  $\ell$  is shown in Fig.2.6. In this case the fraction  $\ell/L$  is always less than unity, which makes it always possible to restore the tether system orbit.

## 2.5 Summary and Conclusions

(a) Unless high specific impulse engines can be used to restore the orbit of the tether platform, tethers cannot advantageously be used to replace part of the chemical propulsion capacity of an OTV.

(b) For a system where the Shuttle is fully loaded with either the largest possible OTV, or a smaller OTV plus additional OMS fuel to reach a tether system at its minimum altitude (compatible with no Shuttle reentry upon release), there is a loss of 4.7% payload per 100 Km of tether.

(c) However, tethers can be used to extend the capacity of a fixed OTV. For a system where the Shuttle carries a Centaur OTV, to a tether system orbiting as high as the maximum OMS fuel will allow, there is gain of 12% per 100 Km of tether.

ORIGINAL PAGE IS  
OF POOR QUALITY

References

- 2.1 "The Use of Tethers for Payload Orbital Transfer," Final Report on Subcontract SV1-52006. Submitted to the SAO by M.I.T. Space Systems Lab, March 22, 1982 (Chapter 3).
- 2.2 Ibid, Sec. 4.2.
- 2.3 Ibid, Appendix 1.
- 2.4 Ibid, Chapter 4.

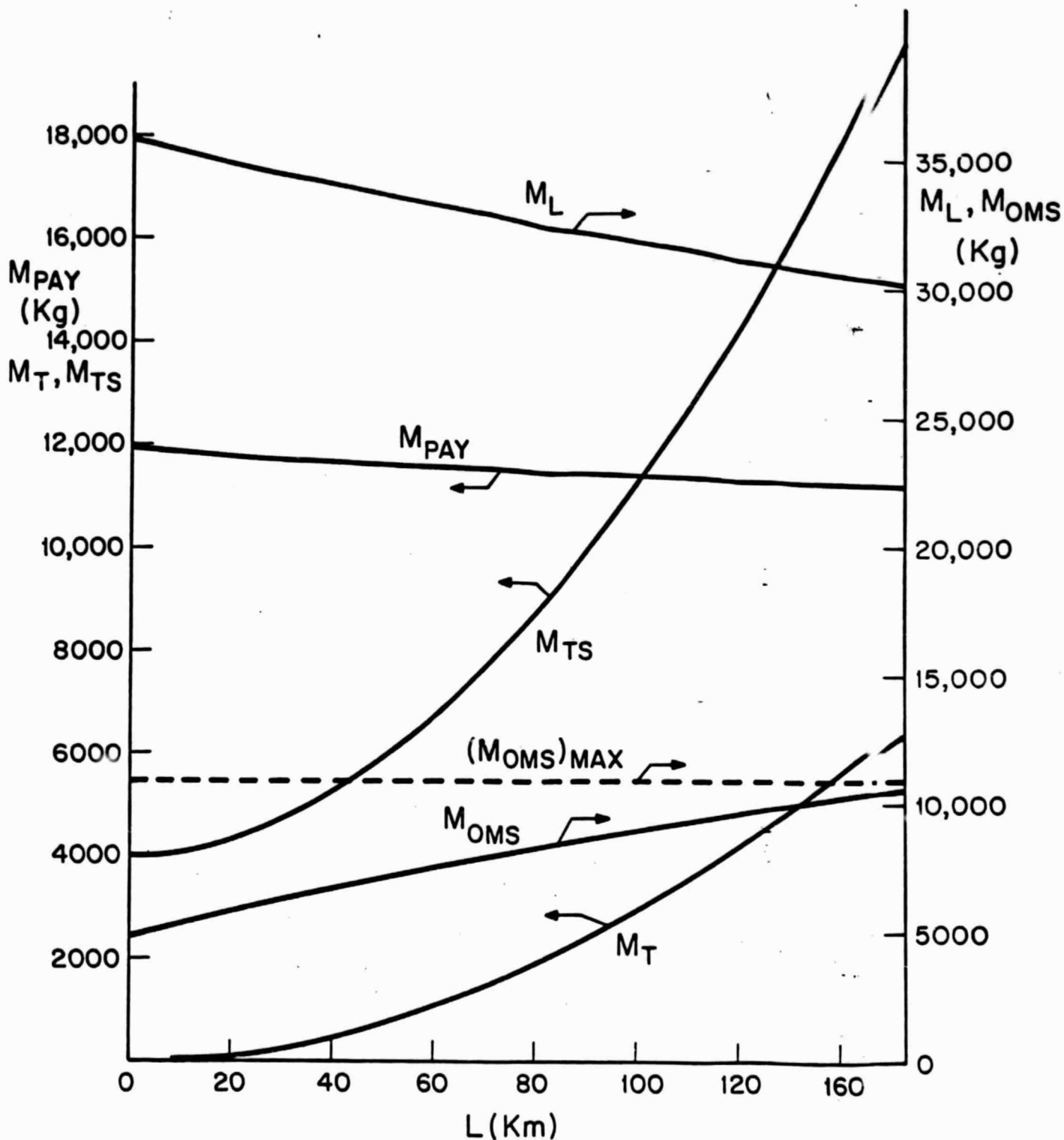


Fig. 2.1 Case with Throw Weight Limited to 40,770 Kg.  
Variation of payload, tether and tether system masses (left scale),  
and of loaded OTV and OMS Orbiter fuel (right scale) with tether  
length. Minimum altitude 100 nm.



ORIGINAL PAGE IS  
OF POOR QUALITY

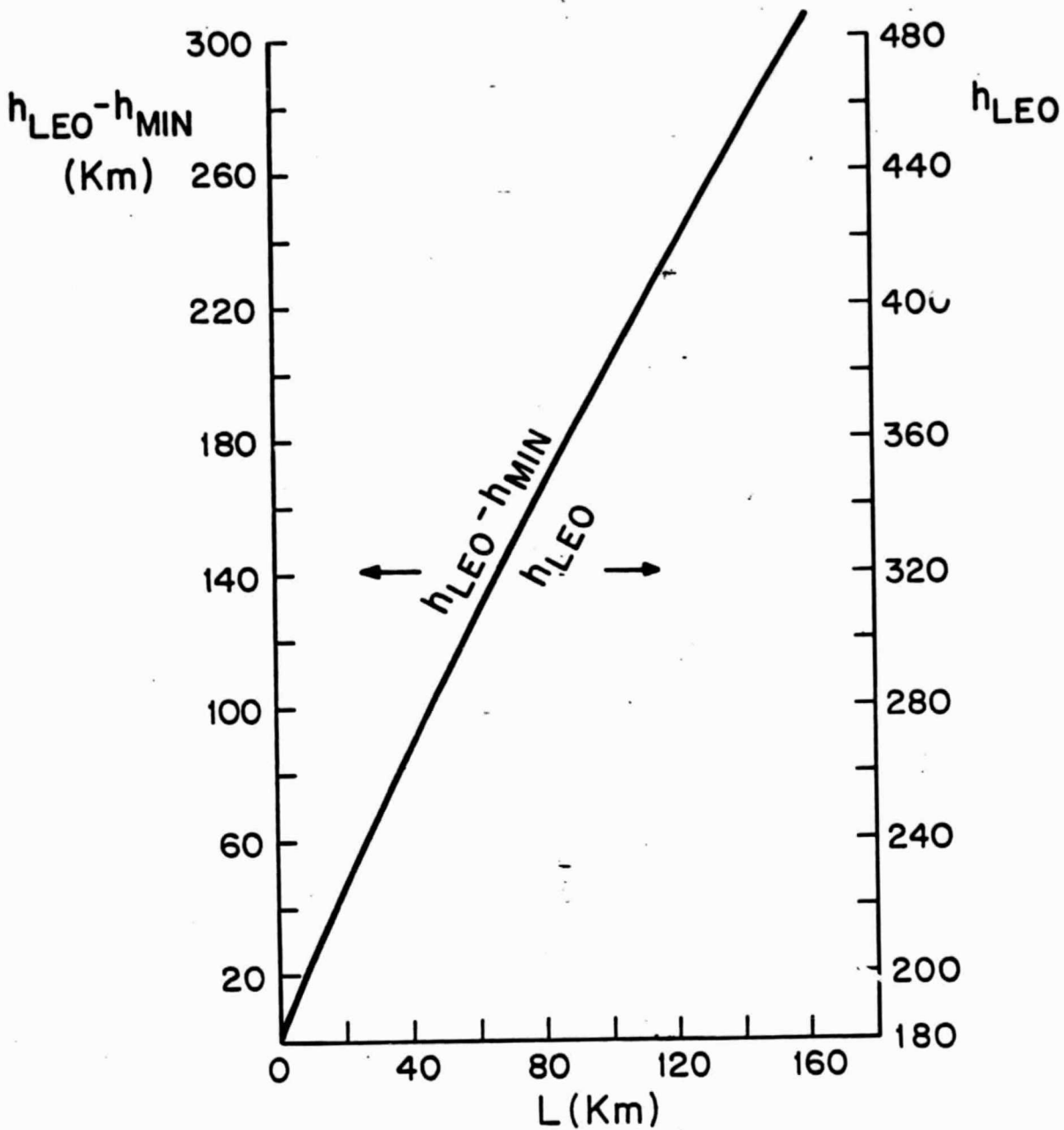


Fig. 2.2 Shuttle Altitude Loss (Left) and Tether Parking Altitude (Right), versus Tether Length (for case with maximum throw weight).

ORIGINAL PAGE IS  
OF POOR QUALITY

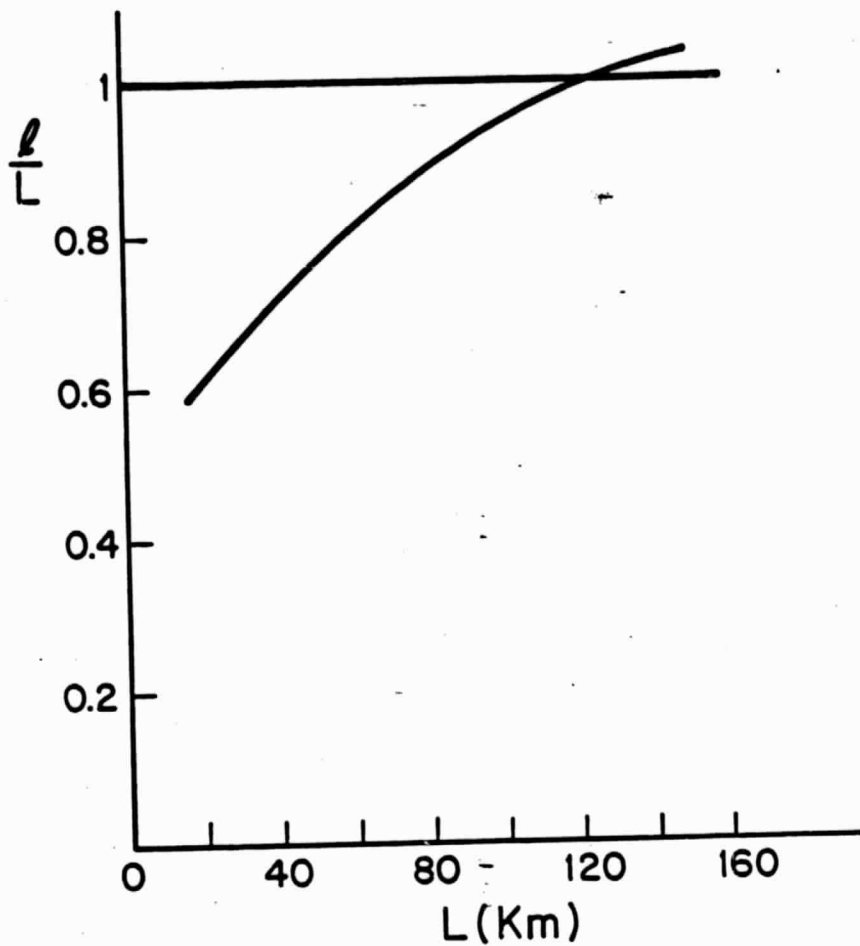


Fig. 2.3 Fraction of Tether Length Left Deployed at Shuttle Detachment (case with maximum throw weight).

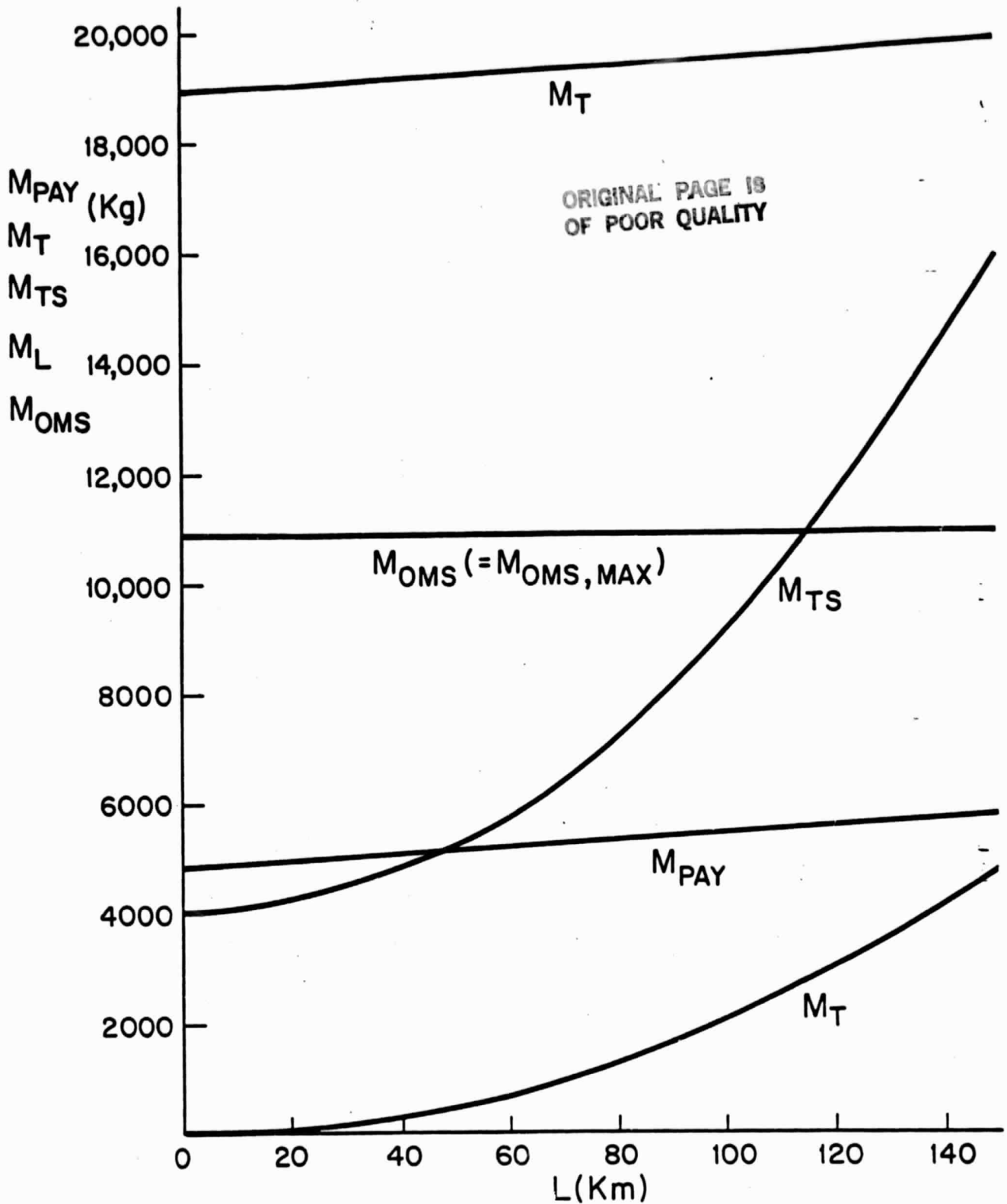


Fig. 2.4 Case with limited OMS fuel, fixed OTV vehicle variation of payload, loaded OTV mass and tether and tether system masses with tether length.

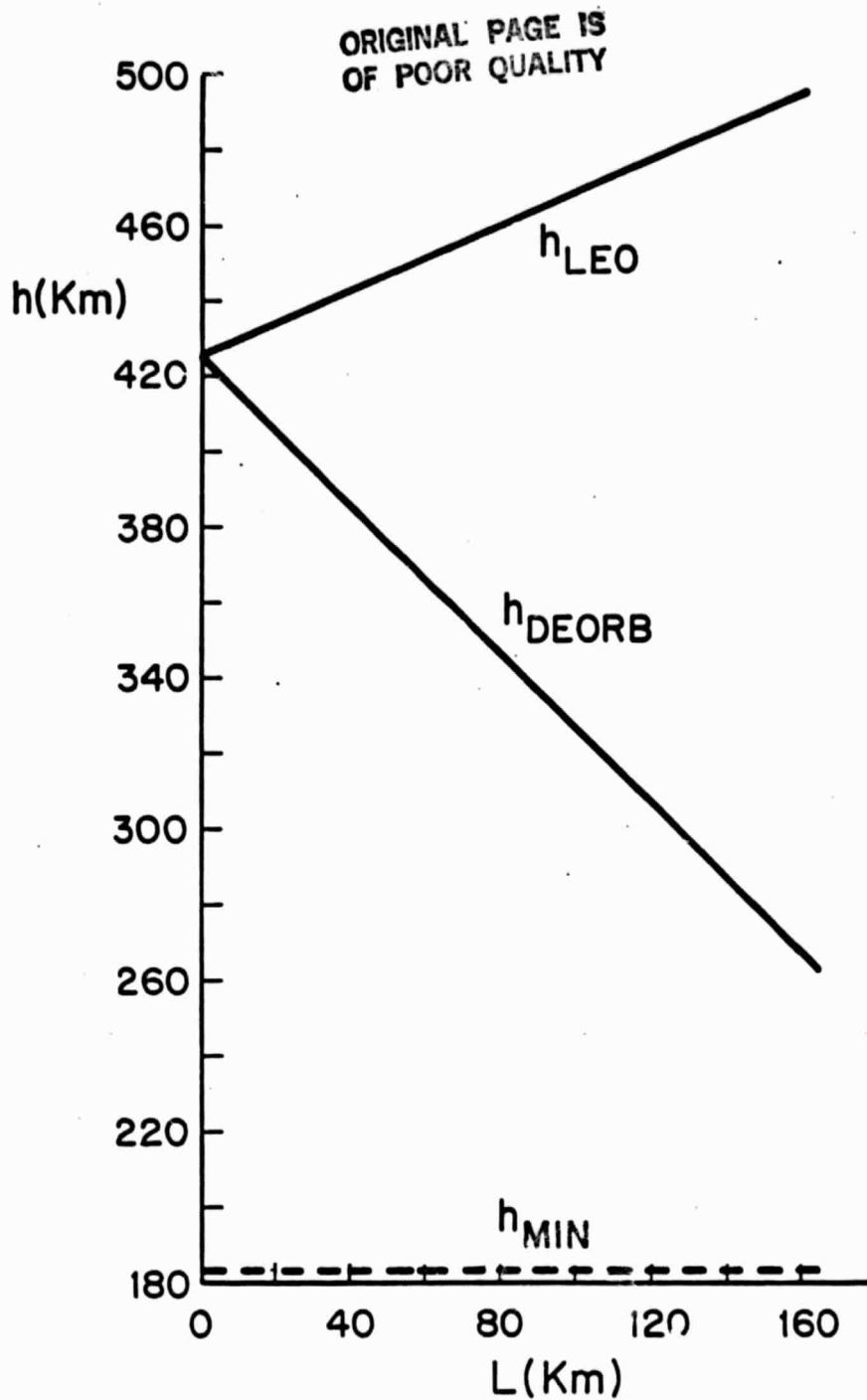


Fig. 2.5 Tether system parking altitude ( $h_{LEO}$ ) and lowest shuttle altitude ( $h_{deorb}$ ) versus tether length for case with fixed OTV, maximum OMS fuel also shown is minimum allowable altitude.

ORIGINAL PAGE IS  
OF POOR QUALITY

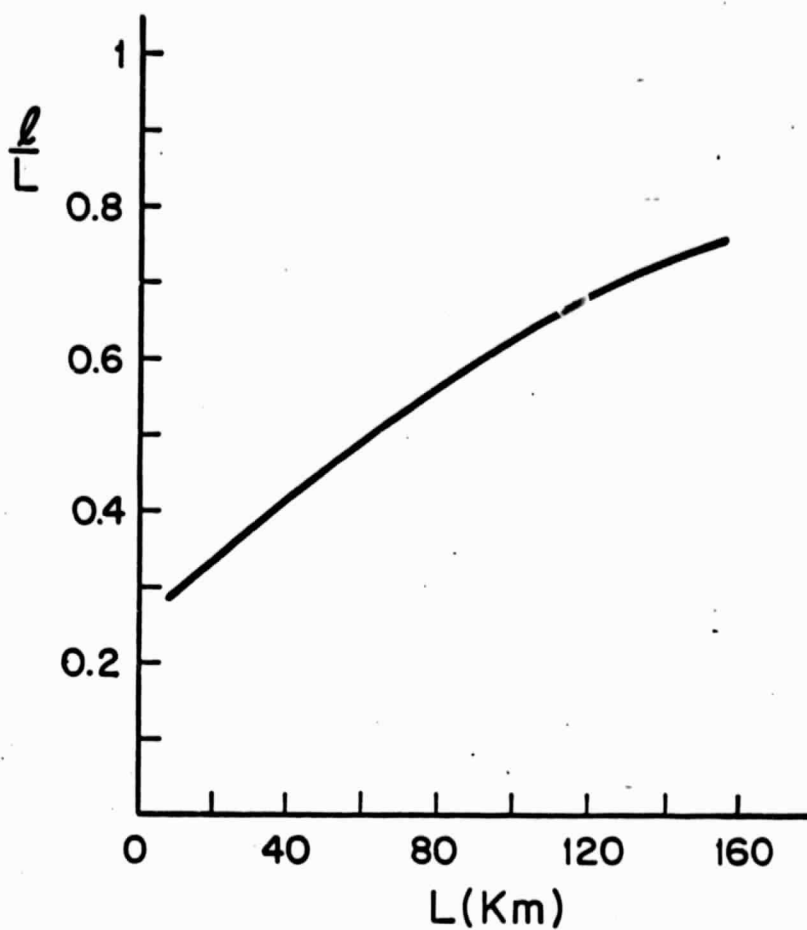


Fig. 2.6 Fraction of tether length left deployed at Shuttle detachment (case with fixed OTV and maximum OMS fuel).

### 3. Shuttle-based Tethers for Deep Space Launch Assist

High energy, deep space missions, such as the Galileo Jupiter mission or the potential Saturn flyby, for instance, stretch to the limit the capabilities of existing launch vehicles. The situation is illustrated in Figure 3.1, where an assortment of vehicle payload-energy envelopes is presented and a few representative mission requirements are shown. The quantity in the abscissa is

$$c_3 = v^2 - \frac{2\mu_E}{r}$$

or twice the total energy in a hyperbolic geocentric orbit ( $c_3 = 0$  would be the Earth-escape condition). The notation (EGA) in some of the missions stands for Earth Gravity Assist, a maneuver that greatly lengthens the flight time. As the figure shows, only the modified wide-body Centaur can accomplish the direct Galileo flight. This is the present baseline for the mission, and it does require development and qualification of the Shuttle-compatible wide-body Centaur.

We examine in this section the possible alternative of extending the capabilities of a less powerful transfer vehicle by means of a tether deployed from the Shuttle in a manner entirely analogous to that discussed in Section 1 of this Report, with the modification that maximum on-board fuel (OMS fuel) and not necessarily maximum throw weight, is the limiting factor. This means that a fixed OTV, smaller than could be accommodated by the Shuttle's limited throw weight capability, is supplemented by an on-board tether facility instead of being replaced by a modified, larger mass OTV. The length of tether to be used is limited by either:

- (a) A minimum post-release Shuttle perigee of 100 n.m., or
- (b) The sum of the OTV and tether facilities exceeding the throw weight limit.

Clearly, the extra boost (if any) to the payload due to this maneuver will be coming from a more efficient use of the OMS fuel in the Shuttle. In a conventional deployment, this fuel would fly the Shuttle as high as possible, the OTV would be released, and the momentum added to the Shuttle itself would be lost. The tether will transfer a part of that momentum to the OTV, while sending the Shuttle to a lower orbit.

3.2 Analysis. Most of the equations and concepts of Section 1 can be directly used in this calculation. A list of Symbols is included here as Table 3.1.

Table 3.1 Notation

$L$	= tether length
$\chi_{cg}$	= for a deployed tether, distance from its lower end to the c.g. of the shuttle-tether-payload system
$\chi'_{cg}$	= same, but to c.g. of shuttle-tether system alone
$R_{LEO}$	= radius to the initial orbit of the shuttle tether-payload system
$R_a$	= apogee of $\chi_{cg}$ of the shuttle-tether system after the payload is released. (Also deorbit radius of Shuttle)
$R_p$	= perigee of $\chi_{cg}$ of shuttle-tether system after the payload is released.
$R_{MECO}$	= radius of Shuttle at MECO.
$R_{OTV}$	= radius of OTV at the end of the fully extended tether.
$R_J$	= radius of Jupiter to the sun.
$R_E$	= radius of Earth to the sun.

- $M_{OMS}$  = total mass of OMS propellant = constant 28,000 lbs.  
 $M_{SH}$  = structural mass of shuttle (empty)  
 $M_{JOTV}$  = total mass of OTV propellant  
 $M_{sOTV}$  = structural mass of OTV (empty)  
 $M_L$  = loaded OTV mass (including payload)  
 $M_{PA}$  = payload mass  
 $M_T$  = tether mass  
 $M_{up}, M_o$  = masses of upper and lower pallets at the tether ends  
 $M_{Tot1}$  = total mass of shuttle-tether-payload system after reaching  
           original orbit  $R_{LEO}$   
 $M_{throw}$  = shuttle throw weight, limited to 90,000 lbs.  
 $V_{Ee}$  = OTV escape velocity from earth (at  $R_{LEO}$ )  
 $\Delta V_{inj}$  = shuttle velocity increment to circularize after MECO  
 $\Delta V_{tr}$  = shuttle velocity increment from standard minimum orbit  
           to desired earth orbit  $R_{LEO}$   
 $\Delta V_{deo}$  = shuttle velocity increment to deorbit  
 $\mu$  =  $1 - e^{-\Delta V/c_{oms}} \approx \Delta V/c_{oms}$   
 $c_{oms}$  =  $g(I_{sp})_{oms}$  = effective jet speed for OMS rockets  
 $c_{OTV}$  =  $g(I_{sp})_{OTV}$  = effective jet speed for OTV rockets  
 $\Delta V_{OTV}$  = OTV velocity increment to escape and enter a heliocentric orbit  
           to Jupiter  
 $c_3$  =  $2E = v^2 - \frac{2\mu_E}{r}$  (twice the total energy in a hyperbolic geocentric  
           orbit).



The OTV, after its release, produces a burn that performs an Oberth maneuver; i.e., it imparts to the vehicle enough excess hyperbolic energy to, not only escape Earth's attraction, but to enter a heliocentric Hohmann transfer orbit to Jupiter as well. The required  $\Delta V$  is easily calculated as

$$\Delta V_{OTV} = \sqrt{(\Delta V_{H_1})^2 + \frac{v_{eg}^2}{1+\lambda}} - (1+\lambda) v_{LEO}$$

where  $\lambda = \frac{L - x_{cg}}{R_{LEO}}$ ,  $v_{eg}$  and  $v_{LEO}$  are the escape and orbital velocities at  $R_{LEO}$  and  $\Delta V_{H_1}$  is the hypothetical first impulse in a heliocentric Hohmann transfer:

$$\Delta V_{H_1} = \sqrt{\frac{\mu_{sun}}{R_E}} \left( \sqrt{\frac{2\rho_J}{\rho_J+1}} - 1 \right)$$

$$\rho_J = R_J/R_E$$

After selecting a tether length  $L$ , the calculation proceeds in an iterative way: a guess is made of  $R_a$ , the Shuttle post-release apogee, as well as of the distances  $x_{cg}$  and  $x'_{cg}$  (see Table 3.1). This is tantamount to guessing the radius  $R_{LEO} = R_a + x_{cg} - x'_{cg}$  to which the assumed full OMS fuel supply will lift the loaded Shuttle. It also allows calculation of the post-release perigee  $R_{p_{min}} = R_{LEO} - 7(x_{cg} - x'_{cg})$ , which should not dip below 100 n.m. These data then can be used to calculate the  $\Delta V$  values for Shuttle injection into parking orbit, for Shuttle transfer to the desired ( $R_{LEO}$ ) orbit, and for eventual deorbiting from the apogee ( $R_a$ ) of the post-release orbit. The calculations are as in Section 1, except the eccentricity  $e$  is zero in this case.

The OTV velocity increment  $\Delta V_{OTV}$  can now be calculated, as shown before, and from the given characteristics of the OTV ( $M_{f_{OTV}}$ ,  $M_{s_{OTV}}$ ,  $c_{OTV}$ ), the payload capacity  $M_{PA}$  can be found. This then allows a first calculation of the loaded OTV mass,  $M_L^{(1)} = M_{PA} + M_{s_{OTV}} + M_{f_{OTV}}$ , and completes the first leg of the iteration. For a separate calculation of  $M_L$ , we first evaluate the tether and tether system masses using the equations of Secs. 1 and 2, and impose the condition that the full OMS fuel  $M_{OMS}$  is burnt:

$$M_L^{(2)} = \frac{M_{OMS} - (M_{Ts} + M_{SH})(\mu_{inj} + \mu_{tr} + \mu_{deorb})}{\mu_{inj} + \mu_{tr}}$$

If  $M_L^{(2)}$  and  $M_L^{(1)}$  do not coincide, a new value of  $R_a$  is selected, and  $\chi_{cg}$  and  $\chi'_{cg}$  are updated using their definitions (see Eq.(12) of Sec.2).

The fixed parameters used in the calculations were:

$h_{min}$	= 182 Km	$c_{OMS}$	= 3,038 m/sec
$M_{up}$	= 2000 Kg	$R_{meco}$	= 6479.3 Km
$M_{OMS}$	= 28,000 lb	$V_{meco}$	= 7796 m/sec
$M_{SH}(\text{empty})$	= 80,000 kg	$\Delta V_{inj}$	= 92 m/sec

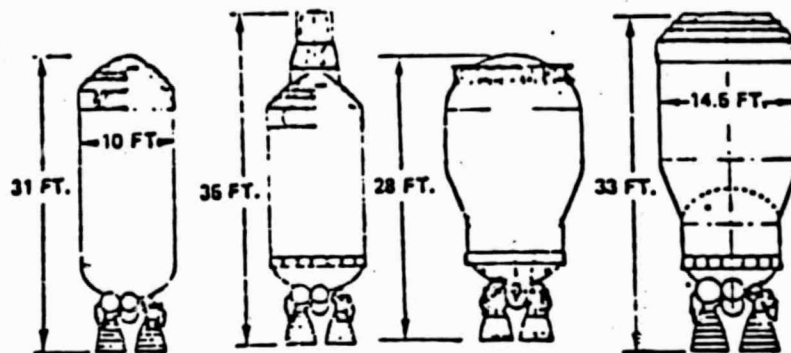
### 3.3 Results

Four different versions of the Centaur vehicle were examined. Their characteristics are listed in Table 3.2. The results are presented graphically versus tether length in Figures 3.2, 3.3, 3.4 and 3.5. In these graphs, the line corresponding to each OTV is truncated at the point where the post-release perigee dips to 182 Km.

Figure 3.2 shows that the payload capability of each of the vehicles examined can be increased by about the same amount (~ 400 Kg) before the

ORIGINAL PAGE IS  
OF POOR QUALITY

Table 3.2 Comparison of Centaur Versions



	D-1T	D-1S	RC	RLTC
Total Dry Weight, lb	4,028	5,018	4,995	5,510
Liftoff Weight, lb	43,776	46,287	59,731	65,000
Installed Length, ft	31	35*	28**	33
Max Diameter, in.	126	126	176	174
Payload to Sync Eq, lb	7,400	4,096*	4,581	4,500
Nominal Solo Flight, hr	6.9	24	30	36
Number of Burns	4	5	5	6
Percentage Existing Hardware	100	85	69	50
Propellant Capacity, lb	30,000	29,000	47,000	52,000
Mixture Ratio	5.0:1	5.8:1	5.8:1	5.0:1
$I_{sp}$ , sec	444	439.8	439.8	444
Dolloff Vented, lb	187	298	468	661
Pressurization, lb Helium	14	18 amb	15 amb	28 cryo
Chilldown and Start Losses, lb $O_2$ & $H_2$	416	175	188	210
ACPS Propellants, lb	482 $H_2O_2$	626 $H_2O_2$	482 $H_2O_2$	690 $N_2H_4$
Computer Memory, k bits	16	24	24	48 (triple)
Guidance Update	N.A.	Ground	Ground	Autonomous
Electrical Power	Batteries	Batteries	Fuel Cell	Fuel Cell
Reliability	0.984 solo	0.951*	0.97 Solo	0.9751
Development Cost, M\$	75	63.3	77.2**	122
Production Unit Cost, M\$	5.2	8.1	8.5	11.9
Launch (Turnaround), M\$	1.1	1.7	0.9	1.2

\* A 22-foot version is included for 35-foot payloads

\*\* With Kick Stage

perigee limit is encountered. In terms of percentage, the largest effect is on the smallest vehicle, the D-1S(R), where a 34% extra is achieved. Notice that, in this calculation, the RC and RLTC versions are always capable of delivering the approximately 2500 Kg Galileo payload, while the D-1S(R) is always below this capability. The D-1T version has a payload capacity of 2000Kg with no tether, but is very close to achieving the required payload with full tether length (172 Km).

These results are, however, put in perspective by Fig. 3.3, where the resulting throw weights are displayed. The larger versions (RLTC and RC) exceed the 40900 Kg limit as soon as the tether system is added to the Shuttle (in fact, the RLTC seems to exceed it even without the tether facility). The smaller vehicles, however, allow lengths on the order of 110-120 Km before this limit is met. With this restriction (which is shown by a mark on the corresponding lines in Fig. 3.2), the payload increase for both the D-1T and the D-1S(R) is 280 Kg. Any future relaxation of the throw weight limit would be clearly beneficial to the tether assist concept. Notice that, although the non-zero mass of the tether facility at zero tether length is clearly visible in the throw weight graphs in Fig. 3.3, no such jump is apparent in the payloads shown in Fig. 3.2. In fact, there is some decrease of payload due to this fixed weight, but it is too small to matter. Basically, this extra weight restricts the achievable Shuttle height, but does not reduce its stored momentum, which is partially imparted to the OTV by the tether. Also, the direct effect of a variation in release height for this interplanetary launch is minimal.

Figs. 3.4 and 3.5 show the evolution of loaded OTV mass and tether-related masses, respectively.

In conclusion, then, a Shuttle on-board tether facility can be used to increase the Galileo payload of the existing Centaur vehicle by some 280 Kg, limited by the gross payload bay load allowable. This figure can be taken as a first approximation for other high energy missions, such as Saturn flyby or Tempel-2 rendezvous.

# STS AND EXPENDABLE LAUNCH VEHICLE ESTIMATED CAPABILITIES

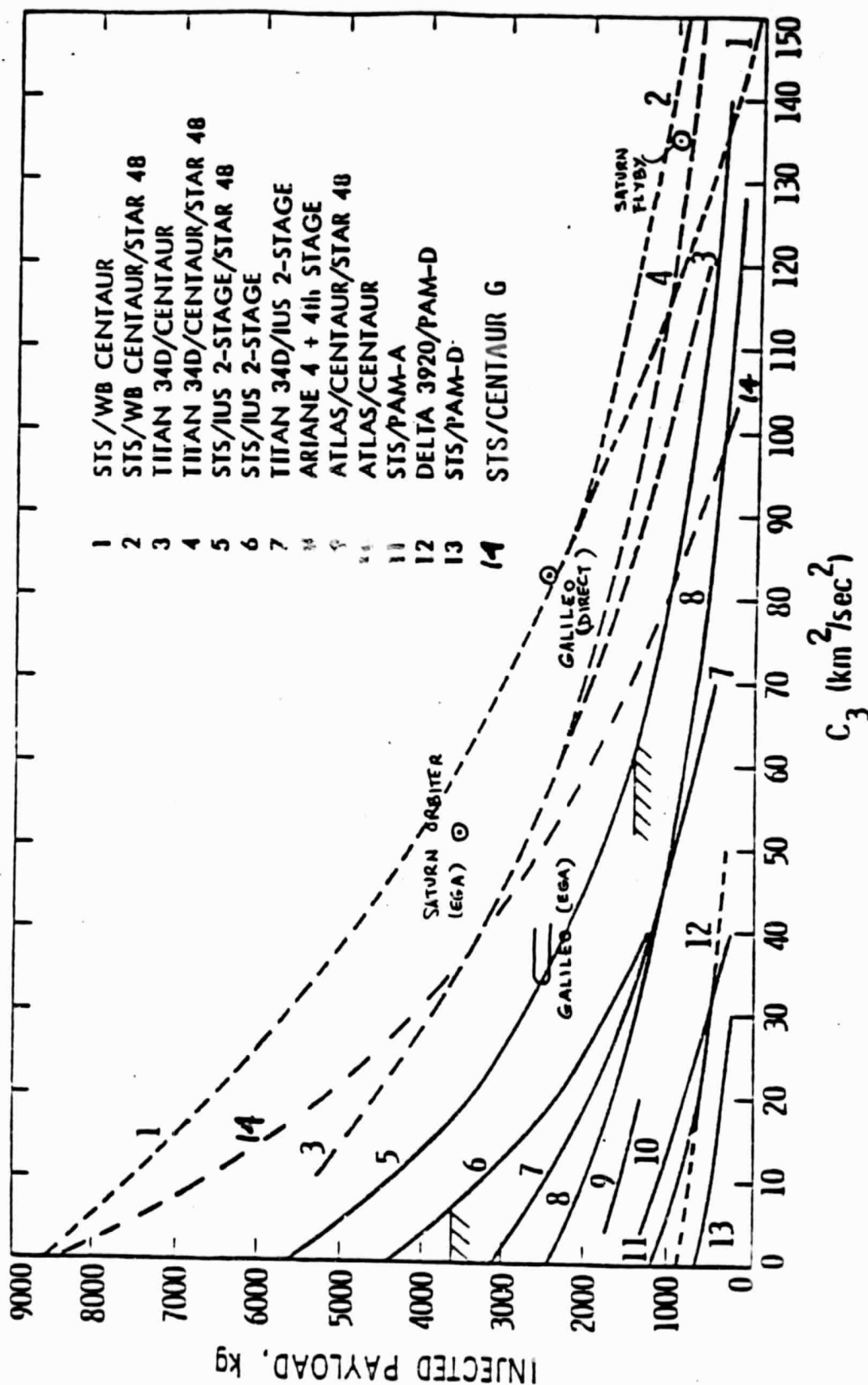


Figure 3.1

ORIGINAL PAGE IS  
OF POOR QUALITY

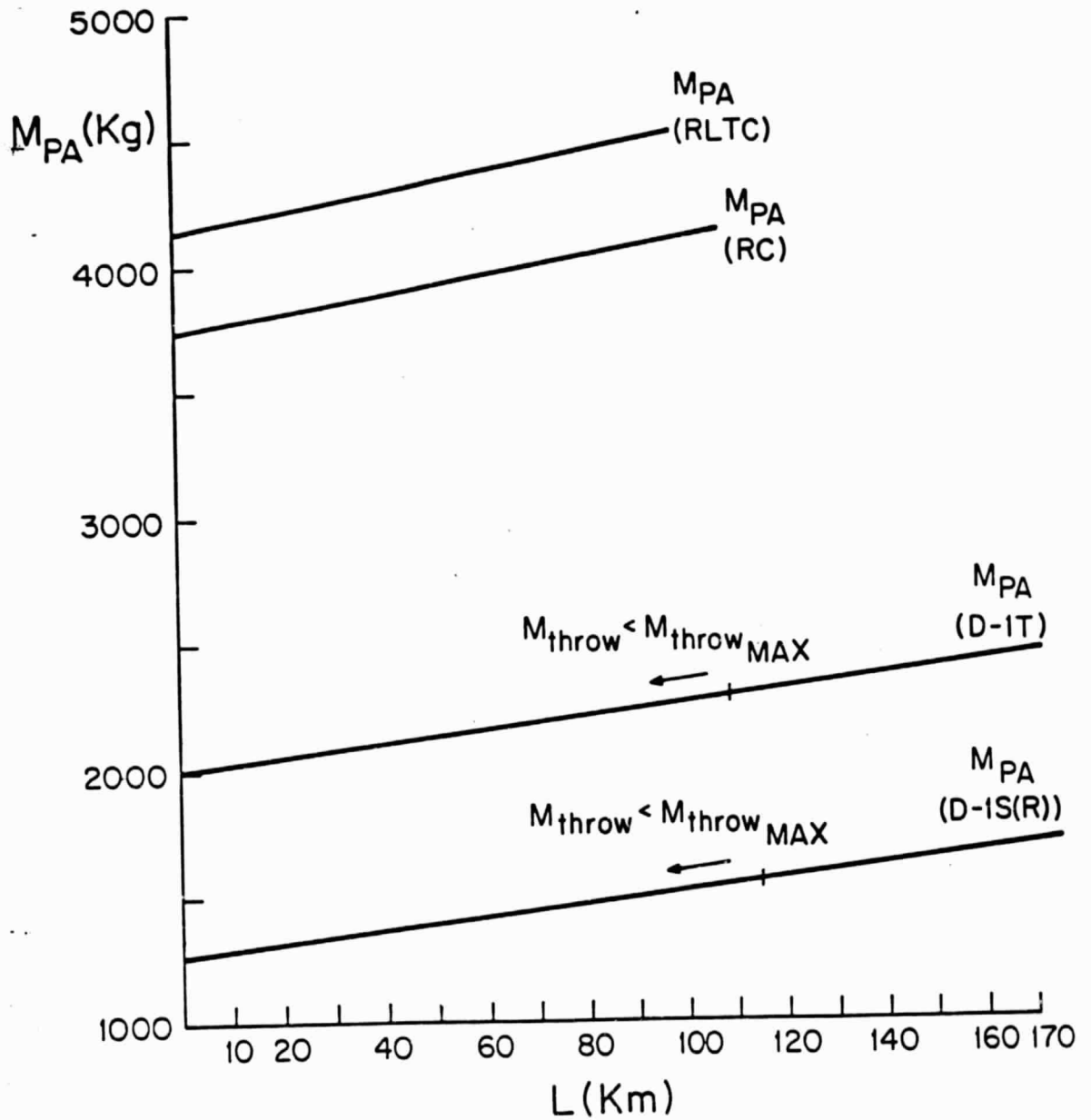


Fig. 3.2 Payload versus tether length

ORIGINAL PAGE IS  
OF POOR QUALITY

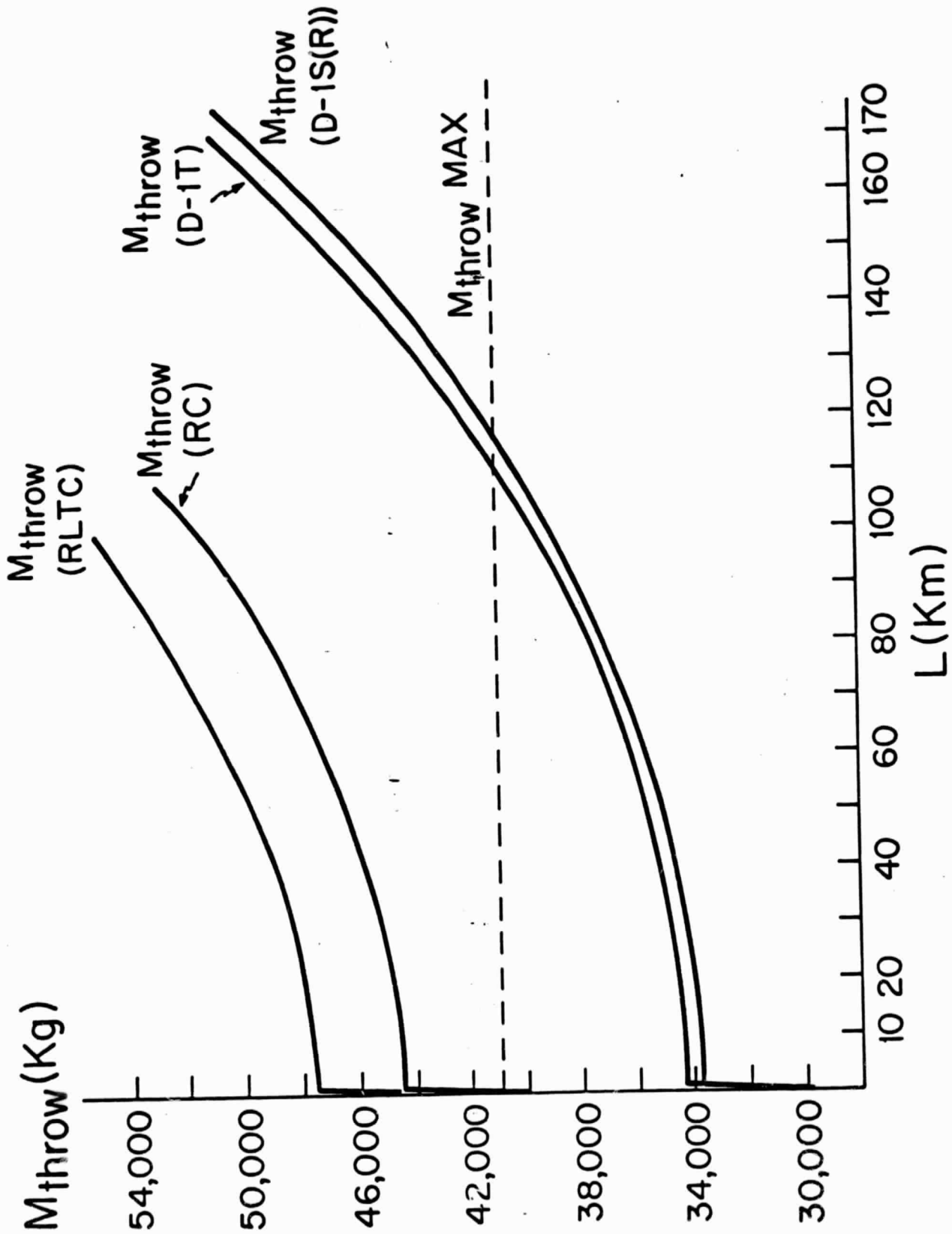


Fig. 3.3 Throw weight versus tether length



ORIGINAL PAGE IS  
OF POOR QUALITY

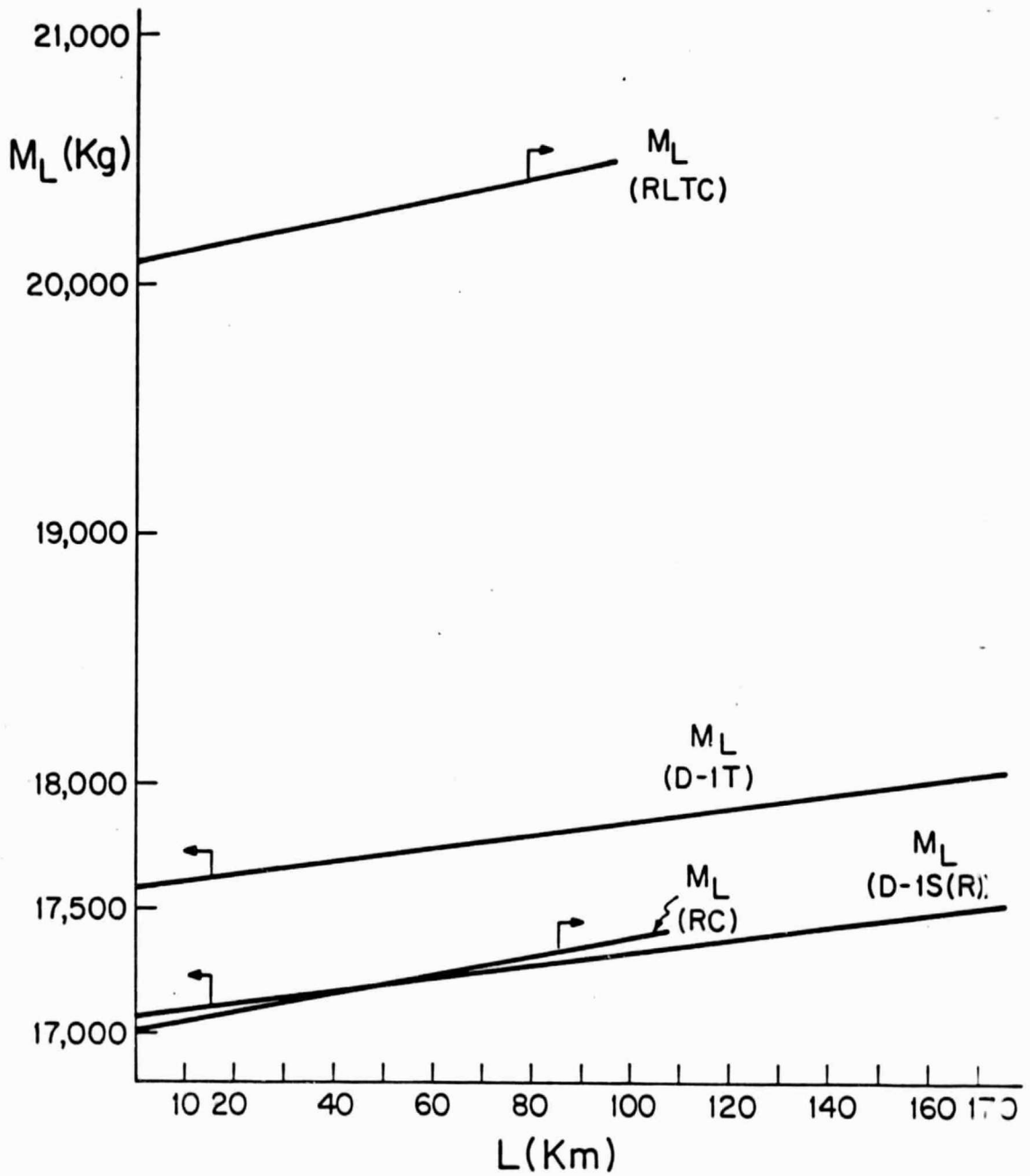


Fig. 3.4 Loaded mass of transfer vehicle versus tether length

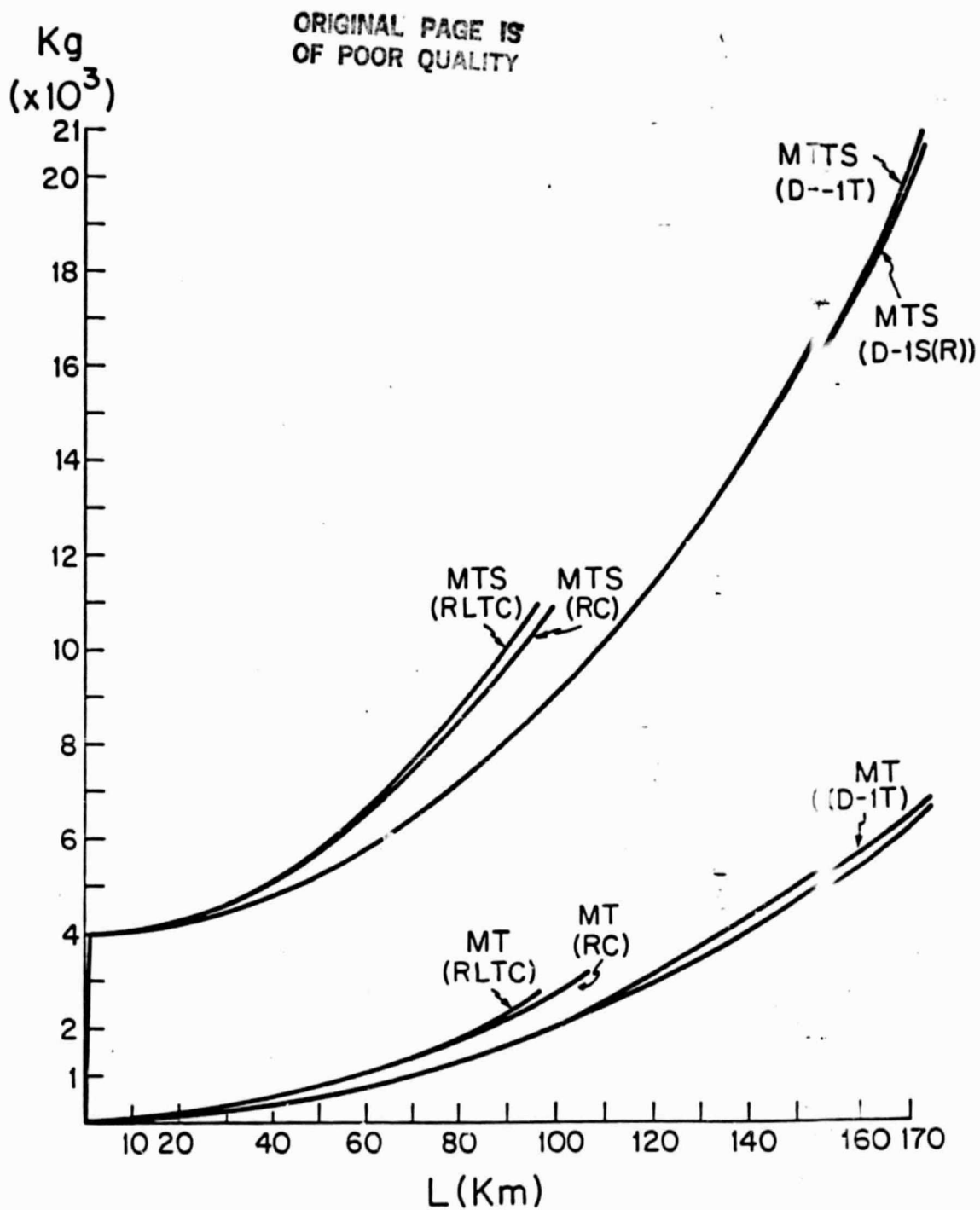


Fig. 3.5 Tether and tether system masses versus tether length

#### 4. Tether Servicing of Intermediate Altitude Satellites

##### 4.1 Introduction

Currently, intermediate altitude satellites (400-1000 Km), such as earth observation satellites (EO), cannot be serviced easily by the Shuttle, since it is only capable of reaching low orbits (LEO). It would be necessary therefore either to send up a repair/refurbishment vehicle from LEO, or use the propulsion unit on the EO satellite itself to bring it down to a reachable orbit. There may be an alternate method of retrieving and servicing satellites, however. This is the concept of deploying a tether from a vehicle or space station in low orbit to rendezvous with the EO satellite in a higher orbit.

A key feature of such a system is the fact that orbits precess about the earth's spin axis because of earth oblateness effects, and this precession rate is a function of orbital altitude. Thus, a station in LEO will precess more rapidly than a satellite at an intermediate (higher) altitude, and the orbital planes will coincide only when the lines of nodes (defined by  $\Omega$ ) are superimposed (assuming identical inclinations). See Figure 4.1. This property can be exploited most effectively if there is a family of satellites to be refurbished at identical orbital inclinations, but different  $\Omega$  and possibly different altitudes (H). A single station could then be used to sequentially service each satellite in turn, by precessing until the orbital planes coincide and retrieving the satellite by means of a tether extended up to the proper altitude.

ORIGINAL PAGE IS  
OF POOR QUALITY

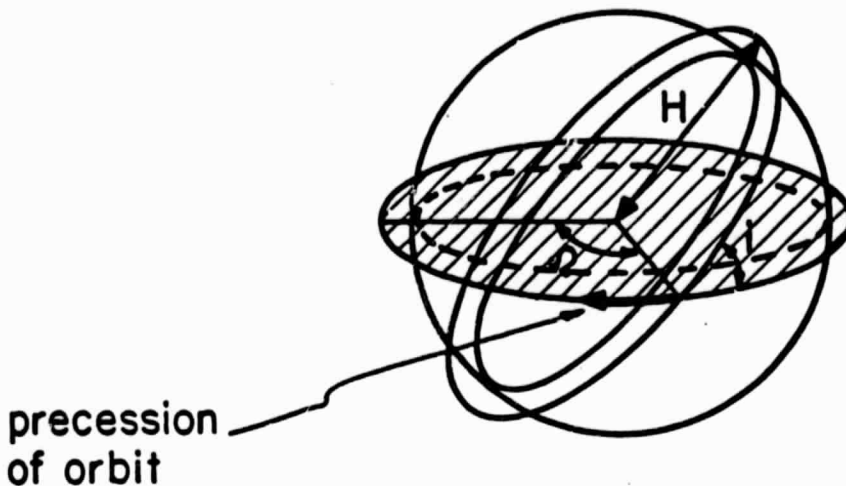


Figure 4.1 Definition of Terms

Two sample systems of practical interest are the following:

- (a) Servicing of sun synchronous, earth observation satellites in high inclination orbits.
- (b) Tending of science or commercial satellites (autonomous material processing, fabrication of pharmaceuticals . . . ) by a manned space station. This would probably be in a low inclination orbit (say  $28.5^\circ$ ).

#### 4.2 Orbital Precession Rates

The precession of the line of nodes of a satellite (per orbit), due to earth oblateness, is given by (Ref.1)

$$d\Omega/\text{orb} = - 3\pi J_2 \left(\frac{R_E}{p}\right)^2 \cos i$$

where  $J_2$  = 2nd order coef. in Legendre series  
For Earth's gravitational potential

$R_E$  = earth radius

$p$  = semilatus rectum =  $r$  (for circular orbit) =  $R_E + H$

$H$  = altitude

$i$  = inclination

To obtain a time rate of precession, this expression must be divided by the orbital period of the satellite in circular orbit at altitude  $H$ :

$$P = 2\pi \sqrt{\frac{r^3}{\mu}} = 2\pi \sqrt{\frac{(R_E + H)^3}{\mu}}$$

with the result

$$\frac{d\Omega}{dt} = - (9.98^\circ/\text{day}) \cos i \left(1 + \frac{H}{R_E}\right)^{-7/2}$$

Figure 4.2 illustrates this relationship of precession rate to altitude for various inclinations. There are a few things to note from this graph:

- All of the precession rates are quite slow, the maximum being only  $\sim 10^\circ/\text{day}$ .
- The greater the inclination, the lower the precession rate.
- The higher the altitude, the lower the precession rate, at any given inclination.
- Sun synchronous satellites are those which precess around the earth, at the same rate as the earth orbits around the sun. This gives a precession rate of  $360^\circ/365 \text{ days} = 0.99^\circ/\text{day}$ . Only satellites with orbital inclinations between  $96^\circ$  and  $100^\circ$  can achieve this precession rate, and the necessary orbital altitude is very strongly dependent on inclination.

The differential precession rate of two orbits of the same inclination, but differing in mean altitude by  $\Delta H$  can be obtained to first order by differentiation of the  $d\Omega/dt$  expression:

$$\frac{d(\Delta\Omega)}{dt} \approx - 34.93 \frac{\Delta H}{R_E} \cos i \left(1 + \frac{H}{R_E}\right)^{-9/2}$$

Also, the angle  $\Delta\phi$  between the orbital planes of the same inclination  $i$ , but with nodal longitudes different by  $\Delta\Omega$  is  $\Delta\phi \approx (\Delta\Omega) \sin i$ . Thus, although the orbital precession is fastest for near-equatorial orbits, the rate of relative rotation of the orbits at their crossing is proportional to  $(\sin i)(\cos i)$ , and is maximum at  $i = 45^\circ$ .

Notice, finally, that the orbital precession rate depends on eccentricity only through the semilatus rectum  $p = a(1-e^2)$ . For any near-Earth orbit of interest,  $e \leq 0.05$  and the effect of eccentricity can be ignored, if the mean radius is used for  $a$ .

ORIGINAL PAGE IS  
OF POOR QUALITY

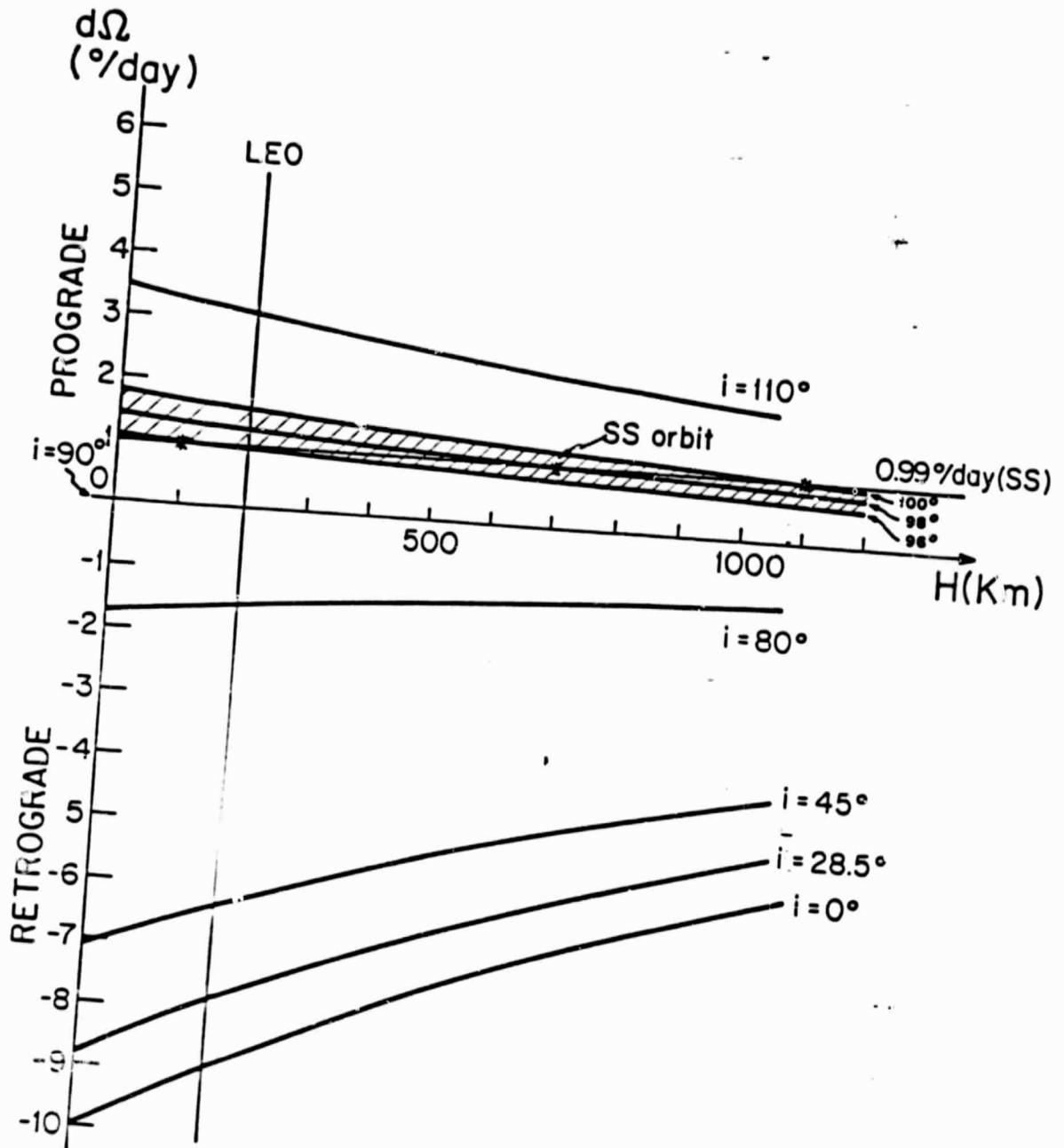


Figure 4.2  $J_2$  Precession Rates

### 4.3 Servicing of Sun Synchronous Satellites

Consider the following system:

- o A sun-synchronous (SS) satellite with  $i = 98^\circ$ ,  $H = 700$  km .
- o A repair/refurbishment retrieval station with tether,  
at  $i = 98^\circ$ ,  $H \approx 400$  km.

Assume both orbits are circular or near-circular. The difference in precession rate between these orbits is (according to Figure 4.2):

$$\Delta (d\Omega/dt) = 0.1^\circ/\text{day}$$

The time period between one superposition of the orbital planes and the following one ( $360^\circ$  later) is:

$$T = \frac{360^\circ}{0.1^\circ/\text{day}} = 3600 \text{ days} \approx 10 \text{ years}$$

This is much too long a period between visits, for this to be a practical system. The problem is due to the fact that the curve of precession rate vs. altitude is very flat for  $i = 98^\circ$ . As a result, the difference in precession rate between the two satellites is simply too small to be practical. Things are different however for lower inclination orbits.

### 4.4 Servicing of Science Platforms in Low Inclination Orbits.

Consider the following system:

- o A science platform in an intermediate orbit with  $i = 28.5^\circ$ ,  
 $H = 800$  km
- o A (manned) space station in LEO with  $i = 28.5^\circ$ , and  $H \approx 400$  km



From Figure 4.2, we can see that we have the following difference in precession rates for these 2 satellites:

$$\Delta\left(\frac{d\Omega}{dt}\right) = -5.8 - (-7.1) = 1.3^\circ/\text{day}$$

With this differential in precession rate, it will take much less time for the ~~two~~ orbits, initially with same  $\Omega$  and  $i$ , to repeat this configuration:

$$T = \frac{360^\circ}{1.3^\circ/\text{day}} \approx 277 \text{ days} \approx 9 \text{ months}$$

If the satellite is at 700 Km, the revisiting time interval is about 1 year. This seems very reasonable as a time period between refurbishment visits for many types of scientific platforms.

If one now augmented the system by putting multiple platforms in orbit at the same inclination ( $i = 28.5^\circ$ ), but different  $\Omega$ , one could use the same space station to sequentially precess into position under each platform and service it. For example, 3 platforms, spaced with  $\Delta\Omega = 120^\circ$  between each, could be serviced - one every 3-4 months. Of course, one could also think of more complicated systems consisting of multiple satellites at multiple altitudes (but all at the same inclination), all being serviced by the same space station which might be kept busy almost full time reeling spacecraft in and out.

An alternative system which may offer advantages would consist of a space station placed in an eccentric orbit selected such that the end of a radial tether deployed outwards from it would travel at apogee at the same altitude and at the same speed as the satellite to be serviced. As was mentioned in an earlier section, this slight eccentricity would not affect significantly the precession rate for a given  $\Delta H$ . However, as we will see in what follows that

this scheme requires a higher mean altitude for the platform in order to maintain a reasonable perigee height. Thus, the time between re-visits must be longer in this case.

In the following sections we explore in a preliminary way the dynamics of these systems, with particular attention to the rendezvous requirements.

#### 4.5 Rendezvous Dynamics for a Circular Platform Orbit

The exact rendezvous dynamics off the end of the tether are beyond the scope of this report, but a few preliminary calculations can help quantify potential problems.

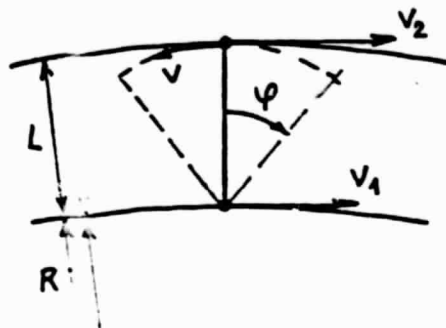
One first requirement for a rendezvous is that the tether station and the satellite must be on the same radial vector from the Earth, at the time of the transfer. Normally, this would not be the case when the orbital planes line up (once every 9-12 months). But this problem can be solved by expending some energy before rendezvous to 'walk' the upper, low-mass satellite along its orbital path so that it is in position when rendezvous is attempted.

This translation along the orbit does not entail a large fuel expenditure, as time can be easily traded off for  $\Delta V$ . A small  $\Delta V_1$  modifies the orbital semimajor axis according to  $\frac{\Delta V_1}{V_1} = \frac{1}{2} \frac{\Delta a}{a}$ , and since the orbital period varies as  $\frac{\Delta T}{T} = -\frac{3}{2} \frac{\Delta a}{a}$ , we obtain  $\frac{\Delta T}{T} = -3 \frac{\Delta V_1}{V_1}$ . As an example, a 10 m/sec impulse will lead to  $\frac{\Delta T}{T} \approx \frac{1}{250}$ , implying that a change in position by half a revolution within the orbit can be performed in  $\sim 120$  orbits (about 1 week). Of course a recircularizing  $\Delta V_2$  of 10 m/sec is necessary at the end of the maneuver, for a total  $\Delta V$  of 20 m/sec.

ORIGINAL PAGE IS  
OF POOR QUALITY

Another requirement for a successful rendezvous is that the velocity of the end of the tether be matched to that of the satellite for a brief moment (~ 1 minute), so that docking can occur smoothly. Assuming the length of the tether can be accurately controlled (radial velocity), there are 2 components that have to be considered: (a) velocity along orbital path; and (b) out-of-plane velocity due to a difference in orbital inclination.

(a) Velocities along orbital path -



$L$  = tether length

In order to match forward velocities, a combination of two techniques can be used. First, the tether is reeled in and out ahead of time so that it starts librating with a fairly large amplitude. Thus rendezvous is timed such that the tether end reaches maximum backswing velocity when the docking occurs. The remaining velocity difference (if any) can then be provided by a propulsion unit on the teleoperator at the end of the tether.

This remaining  $\Delta V$  can be found as follows:

- o if the tether were not librating, the velocity at the tip would be:

$$V_t = (R + L) \omega_1 = (R + L) \sqrt{\frac{\mu}{R^3}}$$

- o but the natural in-plane libration of the tether can be written:

$$\phi = \alpha \sin \sqrt{\frac{3\mu}{R^3}} t, \quad \text{where } \alpha = \text{amplitude of swing}$$

$$\rightarrow |\phi|_{\max} = \alpha \sqrt{3} \sqrt{\frac{\mu}{R^3}} = (V)/L$$

- o at the peak of the backswing, the tether tip velocity is thus:

$$V_t = (R + L) \sqrt{\frac{\mu}{R^3}} - \alpha L \sqrt{3} \sqrt{\frac{\mu}{R^3}}$$

- o this is to be compared with the circular velocity at the higher orbit:

$$V_2 = \sqrt{\frac{\mu}{R+L}} \approx \sqrt{\frac{\mu}{R}} \left(1 - \frac{1}{2} \frac{L}{R}\right)$$

- o the remaining  $\Delta V$  (excess forward velocity of the tether teleoperator) is therefore:

$$\Delta V = V_t - V_2 = L \sqrt{\frac{\mu}{R^3}} \left(-\alpha \sqrt{3} + \frac{3}{2}\right)$$

So by properly choosing  $\alpha$  ( $\alpha = 0.87$  rad), this can be made as small as necessary. The practicality of this 50° libration amplitude needs to be critically assessed. The tether tension is large in the cases considered, so no major dynamic problems are to be expected; however, the tethers are also very massive at these lengths, and reeling them repeatedly in and out may pose operational problems.

A more detailed analysis can be made to estimate the length of time available for docking. At a time  $t$  measured from the peak of the backswing speed, the excess teleoperator velocity is

$$\begin{aligned}\delta V &= \Omega L \left[ \frac{3}{2} - \alpha \sqrt{3} \cos(\sqrt{3}\Omega t) \right] = \\ &= \Omega L \left[ \frac{3}{2} - \alpha \sqrt{3} + \alpha \sqrt{3} \frac{3\Omega}{2} t^2 \right]\end{aligned}$$

where  $\Omega = \sqrt{\frac{\mu}{R^3}}$  and a small angle expansion has been used. It is instructive to represent the behavior of this relative motion in a phase plane with  $\delta V$  as the ordinate and  $\delta x = \int(\delta V)dt$  as the abscissa. Here we assume that the libration has been properly phased, such that maximum backswing velocity occurs at the time of perfect radial alignment.

Fig. 3 shows a schematic of this behavior. Case 2 is that just examined, when perfect rendezvous is achieved at one particular time ( $t = 0$  in our scale). Case 1 corresponds to excess libration amplitude  $\alpha$ ; the teleoperator first passes the satellite at A, slows down and reverses velocity at B, passes the satellite again (this time going backwards) at C, reverses once more at D and passes the satellite one last time at A. The parameters of these key points are easily found to be

Point A:  $\Omega t = \mp \sqrt{3 \frac{\alpha\sqrt{3} - 3/2}{3/2 \alpha\sqrt{3}}}$  ;  $\delta V = 2 \left( \alpha\sqrt{3} - \frac{3}{2} \right) \Omega L$

Points B,D:  $\Omega t = \mp \sqrt{\frac{\alpha\sqrt{3} - 3/2}{3/2 \alpha\sqrt{3}}}$  ;  $\delta x = \pm \frac{2}{3} \frac{(\alpha\sqrt{3} - 3/2)^{3/2}}{(3/2 \alpha\sqrt{3})^{1/2}} L$   
(upper sign for B, lower sign for D)

Point C:  $\Omega t = 0$  ;  $\delta V = - \left( \alpha\sqrt{3} - \frac{3}{2} \right) \Omega L$

ORIGINAL PAGE IS  
OF POOR QUALITY

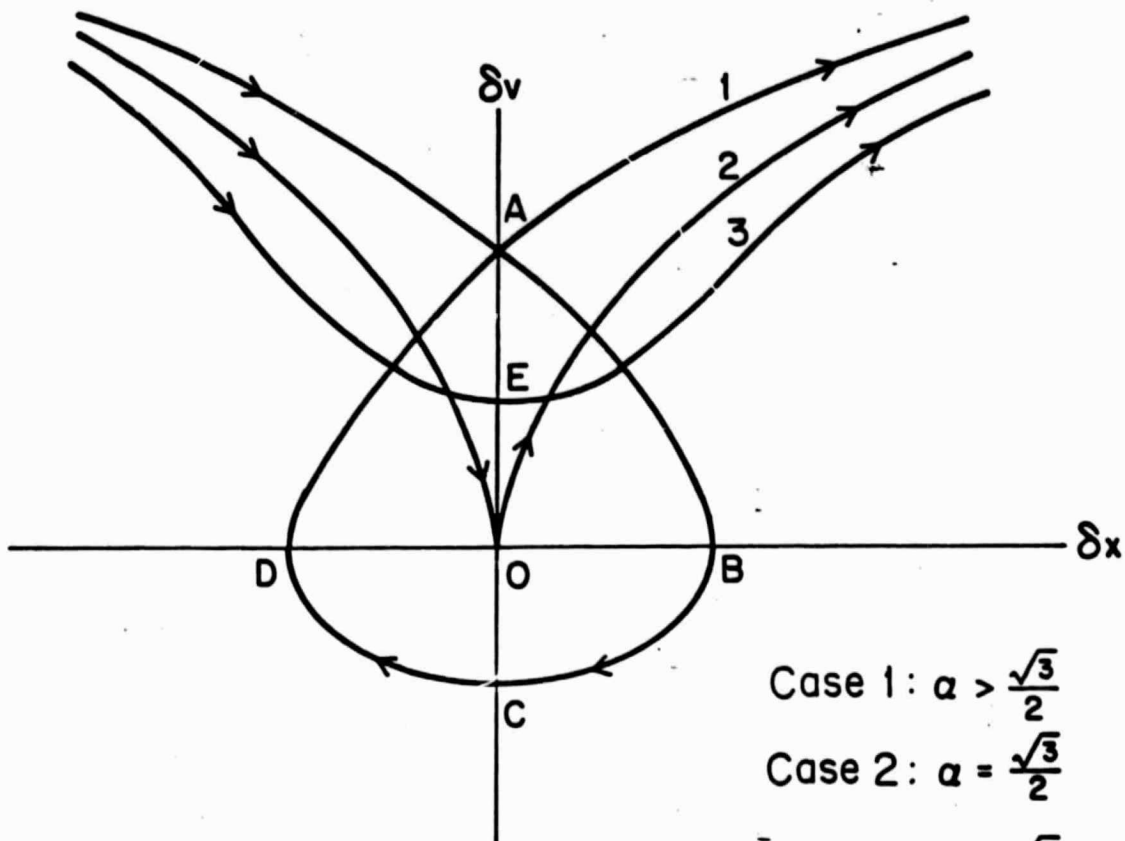


Fig. 4.3 Relative velocity versus separation along flight path between tether teleoperator and satellite.

Curve number 3 corresponds to insufficient libration. The relative velocity remains positive throughout, and the teleoperator passes the satellite at E with  $\delta V = (\frac{3}{2} - \alpha\sqrt{3}) \Omega L$ .

It is clear that a proper choice of excess libration (curve 1) will provide the longest residence time in the vicinity of the satellite. For example, the time to "loop" around the origin (time between passes through point A) is

$$\Delta t = \frac{2}{\Omega} \sqrt{2(1 - \frac{\sqrt{3}}{2\alpha})}$$

and the maximum distance during this looping is OB, or

$$\Delta x = (\frac{2}{3})^{3/2} \alpha\sqrt{3} (1 - \frac{\sqrt{3}}{2\alpha})^{3/2} L \approx \sqrt{\frac{2}{3}} (1 - \frac{\sqrt{3}}{2\alpha})^{3/2} L$$

where  $\alpha = \frac{\sqrt{3}}{2}$  has been used in an insensitive place. Elimination of  $\alpha$  gives the relationship

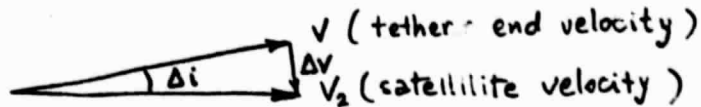
$$\Delta t = \frac{2\sqrt{2}}{\Omega} \left( \sqrt{\frac{3}{2}} \frac{\Delta x}{L} \right)^{1/3}$$

For an orbital angular velocity  $\Omega \approx 10^{-3}$  rad/sec and if the tether length is  $L = 300$  Km, we calculate  $\Delta t \approx 100$  sec if  $\Delta x = 10$  m., and  $\Delta t \approx 50$  sec if  $\Delta x \approx 1.25$  m. This seems to ensure an adequate time in the neighborhood of the satellite, probably sufficient for latching to it using terminal fine control and some form of manipulator arm.

The required excess libration can now be calculated from the  $\Delta t$  expression; we find in our example, for  $\Delta t = 100$  sec,  $\alpha \approx \frac{\sqrt{3}}{2} (1 + 1.2 \times 10^{-3})$ , namely, a 0.12% excess amplitude. The maximum relative velocity during this proximity loop occurs at A; using the given expressions, this is 1.1 m/sec for  $\Delta t = 100$  sec and 0.28 m/sec for  $\Delta t = 50$  sec.

## (b) Out-of-plane velocities -

One can obtain an estimate of how much propulsive capability is necessary on the teleoperator at the end of the tether to take care of small inaccuracies in orbital inclination.



We have:  $\Delta V \approx V_2 \cdot \Delta i$

Thus, for example, to be able to tolerate a  $\Delta i = 1^\circ$ , at  $H = 800$  km, would need the following  $\Delta V$  capability:

$$\Delta V = \sqrt{\frac{\mu}{R}} \cdot \frac{1 \times \pi}{180} = 130 \text{ m/sec.}$$

Alternatively, given a  $\Delta V$  capability, one can easily calculate the allowable error in  $i$ .

Note: The natural out-of-plane libration motion of the tether is not exploited here, because it cannot be excited simply by reeling tether in and out, as with in-plane librations. Of course, an oscillation will occur after a  $\Delta V$  is applied to end of tether as above.

If an inclination error is unavoidable, it appears that only an appropriate propulsion capability on the teleoperator can compensate for it. Assuming for example a  $1^\circ$  inclination error (130 m/sec cross-range relative velocity), the mass of hydrazine required to be burned assuming a teleoperator mass of 1000 kg is

$$M_p = \frac{M \Delta V}{c} = \frac{1000 \times 130}{2230} = 58 \text{ Kg}$$



If this is used in a 2 min. burn, a thrust of 240 lb results.

Hydrazine thrusters in this range are readily available. Note that it would then be necessary to apply a similar stabilizing impulse to eliminate lateral libration after the maneuver is completed.

#### 4.6 Orbital and Rendezvous Dynamics for the Case of an Elliptic Platform Orbit.

Consider a satellite in a circular orbit at  $R_s$ , to be serviced by a platform in an elliptic orbit with apogee at  $R_a$  and perigee at  $R_p$ , by means of a tether of length  $L$ . The relationship between  $R_a$ ,  $R_p$ ,  $R_s$  and  $L$  can be found by expressing that the teleoperator at the tether end reaches  $R_s$  at apogee:

$$R_s = R_a + L \quad (4.6-1)$$

and that it has there the orbital speed  $\sqrt{\mu/R_s}$ . Including the small contribution from the forced libration due to eccentricity (a forward velocity which peaks at apogee with the value  $2e\omega_{orb}L$ ), we can write

$$\sqrt{\frac{\mu}{R_s}} = \frac{R_s}{R_s - L} \sqrt{\frac{\mu}{R_s - L}} \frac{2R_p}{R_s - L + R_p} + 2 \frac{R_s - L - R_p}{R_s - L + R_p} \sqrt{\frac{8\mu}{(R_s - L + R_p)^3}} L$$

If we expand to 2nd order in  $L/R_s$  and  $(R_s - R_p)/R_s$ , this expression can be reduced to

$$\frac{R_s - R_p}{R_s} \approx 7 \left(\frac{L}{R_s}\right) - 6 \left(\frac{L}{R_s}\right)^2 \quad (4.6-2)$$

(notice that without the libration contribution the (-6) coefficient would have become (-30), which amounts in typical cases to a 3/4% difference).

Then perigee  $R_p$  for the platform is to be selected on the basis of the usual tradeoff between performance and lifetime. In this application, a lower perigee would allow more rapid differential orbital precession, as well as lower  $\Delta V$  for each Shuttle visit, but would eventually lead to unacceptably high drag. We take here the approach of selecting a perigee height that would guarantee the same orbital lifetime as a circular orbit at 400 Km altitude, a value that has been found to be a good compromise in space station studies.

From the theory of parameter perturbations (Ref. 4.1), and after averaging over one orbit, the rates of change of semimajor axis and eccentricity due to a specific force  $f$  along the trajectory are

$$\begin{cases} \frac{da}{dt} = 2f \frac{a^{3/2}}{\sqrt{\mu}} \\ \frac{de}{dt} = fe \sqrt{\frac{a}{\mu}} \end{cases}$$

and, by division,

$$\frac{d \ln e}{d \ln a} = 1/2$$

and since  $R_p = a(1-e)$ ,

$$\frac{dR_p}{dt} = (1-e) \frac{da}{dt} - a \frac{de}{dt} = \left(1 - \frac{3e}{2}\right) \frac{da}{dt}$$

Given the normal drag uncertainties, we will simply use  $\frac{dR_p}{dt} \approx \frac{da}{dt}$  for the rate of perigee variation. Following Ref. 4.2, with minor simplifications, the effect of drag on semimajor axis is

$$\frac{da}{dt} \approx -2 \sqrt{\mu a} \rho_p \frac{AC_D}{2M} e^{-\frac{ea}{h}} \left[ I_0\left(\frac{ea}{h}\right) + 2e I_1\left(\frac{ea}{h}\right) \right] \quad (4.6-3)$$

where  $\rho_p$  is the air density at perigee,  $A$  is the frontal area,  $C_D$  the drag coefficient, and  $M$  the mass of the vehicle,  $h$  is the local atmospheric scale height, defined by

$$\rho \approx \rho_p e^{-\frac{R-R_p}{h}} \quad (4.6-4)$$

and  $I_0$  and  $I_1$  are the Bessel functions of imaginary argument.

Notice that, although  $e \ll 1$  in our case, the group  $\frac{ea}{h}$  is not small.

Using the typical scale height  $h \approx 40$  Km (valid at about 400 Km altitude),

$$\frac{ea}{h} \approx 0.02 \times \frac{7000}{40} = 3.5$$

This allows us to use the asymptotic approximations (for  $x \gg 1$ )

$$e^{-x} I_0(x) \approx e^{-x} I_1(x) \approx 1/\sqrt{2\pi x}$$

and, neglecting  $2e$  vs.  $1$ ,

$$\left(\frac{da}{dt}\right)_{\text{elliptic}} \approx -\sqrt{\frac{\mu h}{2\pi e}} \frac{\rho_p AC_D}{M} \left(\frac{ea}{h} \gg 1\right) \quad (4.6-5)$$

On the other hand, for a circular orbit, from Eq. (4.6-3)

$$\left(\frac{da}{dt}\right)_{\text{circ.}} = -\sqrt{\mu a} \frac{\rho_p AC_D}{M} \quad (e = 0) \quad (4.6-6)$$

Thus, the elliptic orbit will have the same lifetime as the circular orbit if their respective perigee densities are related as

$$\frac{(\rho_p)_{\text{ell.}}}{(\rho_p)} = \sqrt{2\pi \frac{ea}{h}} \quad (4.6-7)$$

which leads to a perigee altitude given by

$$R_p = R_c - h \ln \left( \sqrt{2\pi \frac{ea}{h}} \right) \quad (4.6-8)$$

Taking  $R_c = 6370 + 400$  Km,  $h = 40$  Km,  $e = 0.02$ ,  $a \approx R_c$ ,

we calculate  $R_p = 6370 + 340$  Km - or altitude  $h_p = 340$  Km.

Once the station perigee is fixed, the tether length  $L$  follows from the velocity condition already derived (Eq. 4.6-2). For  $h_p = 340$  Km, Table 4.1 lists the results for various altitudes of the satellite to be serviced.

Table 4.1. Tether Length, Station Apogee and Station Mean Altitude versus Satellite Altitude (all for  $h_p = 340$  Km)

$h_s$ (Km)	500	600	700	800	900
$L$ (Km)	22.9	37.3	51.0	66.2	80.8
$h_a$ (Km)	477	564	648	734	820
$\frac{1}{2}(h_a + h_p)$ (Km)	394	452	494	537	580

Notice the short length of the required tethers. This is a definite advantage for the eccentric platform scheme, together with the fact that no large amplitude induced libration is required. On the other hand, the mean altitude (4th row in Table 4.1) is relatively large for each satellite radius. This has two unfavorable consequences;

- (a) A reduction of the differential precession rate.
- (b) An increase of the  $\Delta V$  required to reach the station from, for instance, the Shuttle parking orbit.

Regarding the first point, the re-visiting period is listed in Table 4.2 for the same conditions as Table 4.1:

$h_g$ (km)	500	600	700	800	900
Re-visit time (days)	923	687	507	409	346

Table 4.2

With respect to the second point, notice that the least total  $\Delta V$  required to transfer from a parking orbit at  $R_o$  (with orbital velocity  $v_{co}$ ) to one with apogee  $R_a$  and perigee  $R_p$  is, to first order

$$\Delta V \approx v_{co} \frac{R_a + R_p - 2R_o}{4 R_o} \quad (4.6-9)$$

so that reaching the  $(R_p, R_a)$  orbit involves the same fuel expenditure as reaching a circular orbit at  $R_c = \frac{R_a + R_p}{2}$ .

With reference to the last row of Table 4.6-1, this means an "equivalent" circular orbit of 494 Km for a satellite at 700 Km altitude, for example. Such high orbits strain the payload capacity of the present Shuttle.

4.7 Logistics of Servicing. Once the satellite is engaged by the tele-operator, at least two options are available.

(a) Retrieve the tether with the satellite for refurbishment on the space station. This implies a minimum of a few days to weeks before the satellite can be returned to its altitude, and so a relatively large change in line-of-nodes orientation will result (10-30°). This may or may not be critical, depending on the application. If the system being serviced consists of a constellation of identical, equally spaced (in longitude)

to schedule maintenance such that each satellite is retrieved, serviced and returned to the next longitude, where the next satellite is now picked up for service.

(b) Alternatively, the teleoperator could be upgraded to a repair station, possibly manned, and the servicing operations could be all performed while the satellite is connected to the tether, but at its own altitude. This would have the effect of saving one full up-down tether cycle (with the associated savings in energy and system wear), and would materially reduce the time to satellite redeployment. The change in orientation of the line of nodes may then be only a few degrees, and may be tolerable for most systems.

References

- 4.1 Kaplan, M.H., Modern Spacecraft Dynamics & Control, John Wiley & Sons, 1976, p 356.
- 4.2 Mueller, G.E. and Spangler, R., Communication Satellites, John Wiley & Sons, 1964, p 125.